4 RESULTS

4.1 Preparing conditions for co-immunoprecipitation and expression of a soluble gpUS6

The aim of this thesis was to broaden the understanding of gpUS6- and ICP47-mediated inhibition of peptide translocation by TAP. Using gpUS6 and ICP47 as tools, elucidation of TAP structure and function was to be achieved. Before analysis of gpUS6-TAP interaction could be started, testing of anti-gpUS6 polyclonal antisera and construction of a functional soluble gpUS6 (gpUS6sol) had to be accomplished.

The glycoprotein US6 is a an ER (endoplasmic reticulum) resident 21 kDa type I transmembrane protein, consisting of a small cytosolic tail, a single transmembrane segment (TMS) and a major N-terminal lumenal part (Fig. 4.1). The single glycosylation site in the gpUS6 sequence is used (Hengel et al., 1997) but not relevant for gpUS6 function (Kyritsis et al., 2001). The ectodomain of gpUS6 has been shown to retain the ability to bind to and inhibit TAP function (Ahn et al., 1997; Hewitt et al., 2001; Kyritsis et al., 2001), implying that the cytosolic tail and the TMS are dispensable for gpUS6-mediated TAP inhibition.

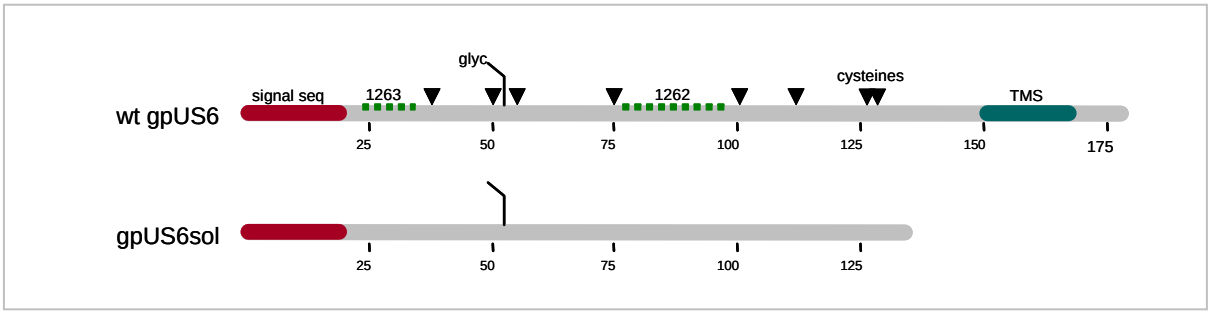

Fig. 4.1 Features of gpUS6.

The protein length of gpUS6 and gpUS6sol are depicted. The peptides against which anti-gpUS6 antisera were raised are indicated as green dotted lines. Cysteine residues are shown as black triangles.

4.1.1 Testing of anti-gpUS6 polyclonal rabbit antisera

Anti-gpUS6 polyclonal rabbit antisera were raised against two gpUS6-specific peptides called 1263 (aa 20-30) and 1262 (aa 77-95) (Fig. 4.1). The specificity for gpUS6 was demonstrated by Western blot (data not shown), before the antisera were analyzed by immunoprecipitation (IP) of metabolically labeled cell lysates. The anti-gpUS6 antisera were tested for co-

immunoprecipitation of TAP, since they were produced for gpUS6 binding studies on TAP. For this purpose stably *US6*-transfected TAP deficient CMT64.5 cells were infected with human TAP1 (hT1) and human TAP2 (hT2) expressing rVV. The cells were lysed with a mild detergent, digitonin, which allows the maintenance of stable TAP-gpUS6 complexes also in cell lysates (Hengel et al., 1997).

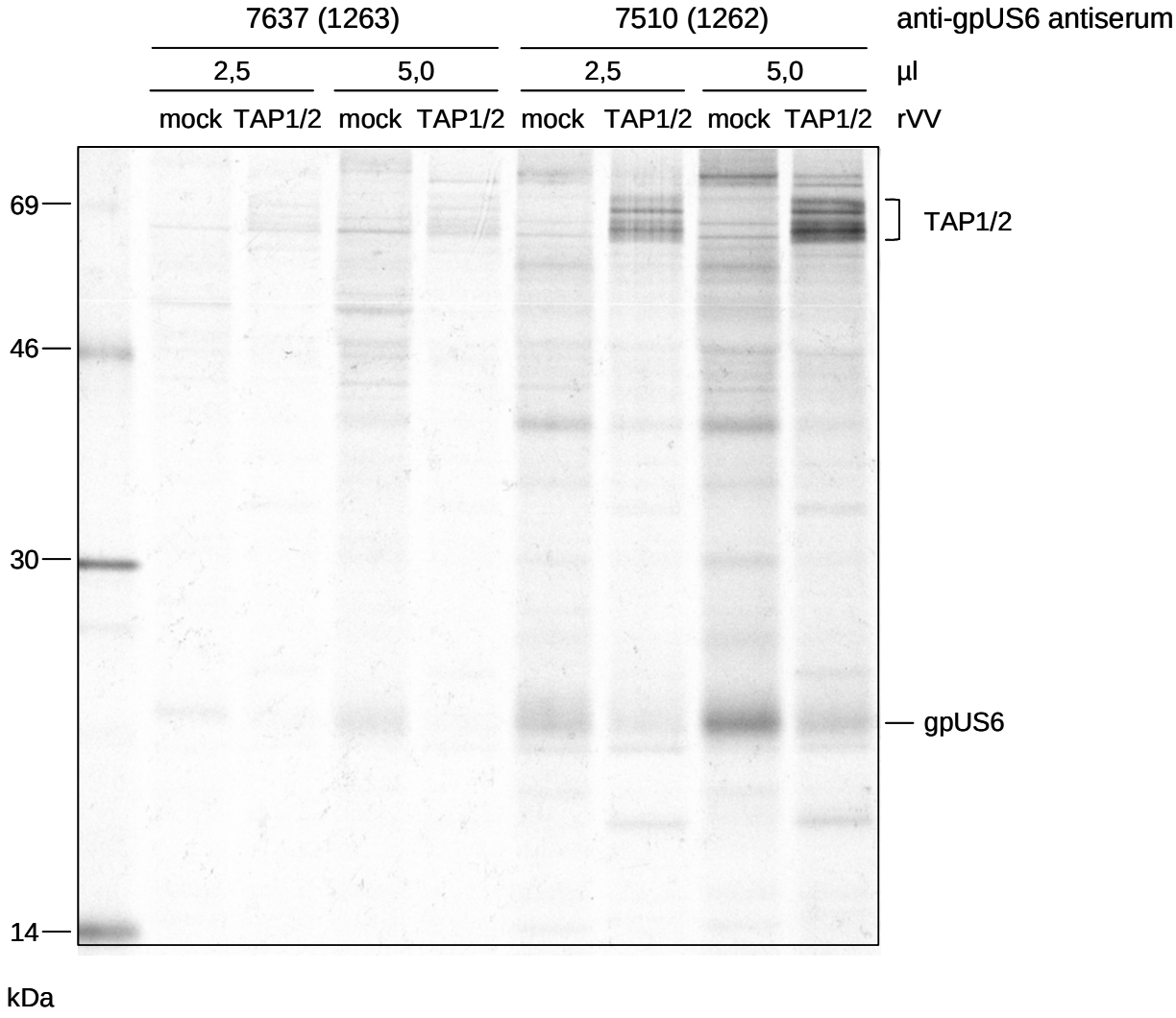

Fig. 4.2 Testing anti-gpUS6 antisera by co-IP.

CMT64.5-*US6* cells were mock treated or infected with human TAP1 and human TAP2 expressing rVV with an MOI of 5. At 15h p.i. cells were metabolically labeled for 1h. Cell lysis was performed by IP lysis buffer containing 1% digitonin. gpUS6 was precipitated by antisera as indicated. Immunocomplexes were collected by PAS. Precipitated proteins were separated by a 10-13% gradient SDS-PAGE. The gel was dried and exposed to an autoradiography X-ray film for 24h. The molecular weight marker is shown on the left side.

Both antisera precipitated gpUS6 (Fig. 4.2), however, the anti-gpUS6 antiserum 7510 (1262) precipitated gpUS6 noticeable more efficient than the 7637 (1263) antiserum. The reduced

levels of gpUS6 precipitated from infected cells demonstrate the host protein synthesis shut-off function by VV-expression (prominent by long VV-infection). TAP subunits were barely detectable with the 7637 antiserum, while the 7510 antiserum co-precipitated TAP effectively, though, with a strong background level. For analysis of TAP mutants a distinct separation of TAP subunits was essential. Therefore, anti-gpUS6 antibodies were purified from the highly sensitive 7510 antiserum using peptide affinity chromatography. The purified fraction E2 contained most of the specific antibodies and was tested by co-IP.

The anti-gpUS6 antibody purification was successful as most of the background seen with the 7510 antiserum was absent when using the anti-gpUS6 E2 fraction, while the ability of strong co-precipitation of TAP subunits was maintained (Fig. 4.3). Another result of this assay, is the observation that gpUS6-TAP complexes can only be precipitated by anti-gpUS6 antibodies and not by anti-TAP1 (7507) or -TAP2 (7509) antibodies. TAP specific antibodies however, precipitate the complete dimeric TAP complex and not only the specifically recognized subunit. E2 (7510) was applied for all further gpUS6 binding analysis to TAP in metabolically labeled lysates.

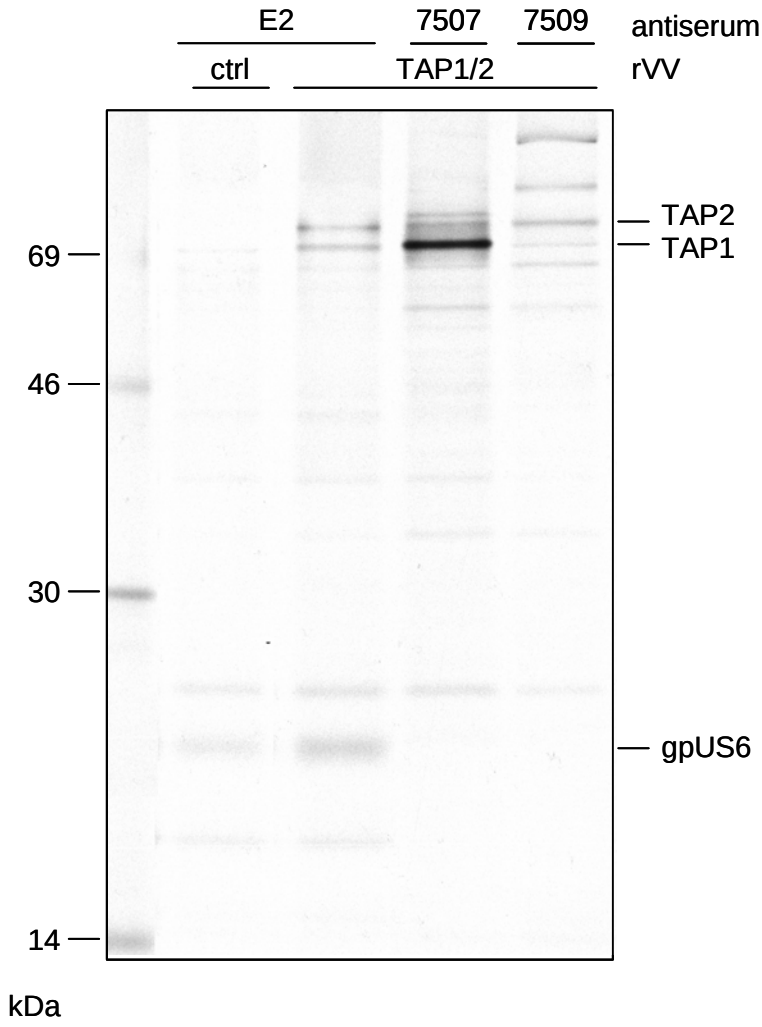

Fig. 4.3 Testing purified anti-gpUS6 antibodies by co-IP.

CMT64.5-*US6* cells were infected with human TAP1 and human TAP2 expressing rVV or with a control (ctrl)-rVV (ICP47-rVV) with an MOI of 5. At 15h p.i. cells were metabolically labeled for 1h. Cell lysis was performed by IP lysis buffer containing 1% digitonin. gpUS6 was precipitated by 12µl E2 (7510), TAP1 and TAP2 were precipitated by 5µl 7505 and 7509 rabbit antiserum, respectively. Immunocomplexes were collected by PAS. Precipitated proteins were separated by a 10-13% gradient SDS-PAGE. The gel was dried and exposed to an autoradiography X-ray film for 24h. The molecular weight marker is shown on the left side.

4.1.2 Expression of gpUS6sol

To discriminate between strictly lumenal and possible transmembrane interactions between gpUS6 and TAP, a soluble truncated mutant of gpUS6 (aa 1-139) was constructed (Fig. 4.1). gpUS6sol possess a glycosylation site, which indicates proper translocation of gpUS6sol into the lumen of the ER. To assess this, CV1 cells were infected with gpUS6sol-rVV. The cells were metabolically labeled prior to lysis and gpUS6 was precipitated by anti-gpUS6 antiserum. Precipitated proteins were subjected to Endo H digest for deglycosylation.

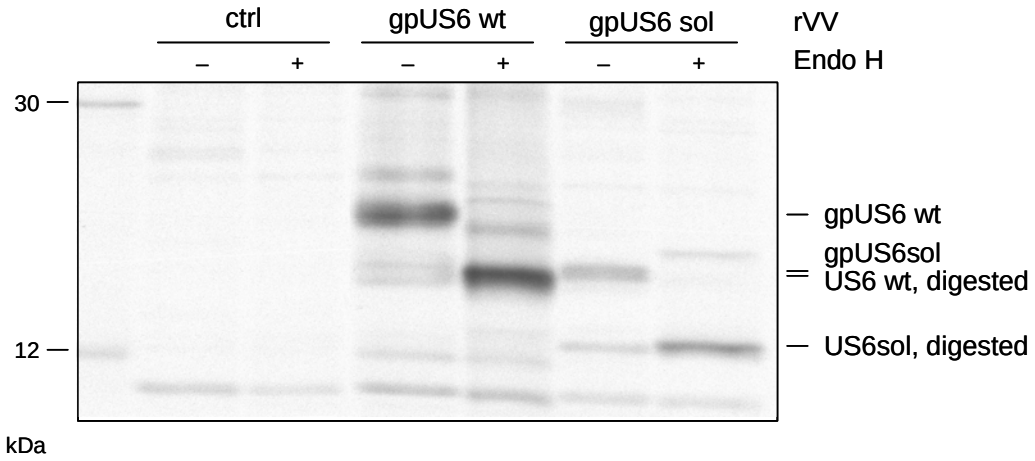

Fig. 4.4 Analyzing glycosylation of gpUS6sol.

CV1 cells were infected with gpUS6-rVV, gpUS6sol-rVV or with a control (ctrl)-rVV (ICP47-rVV) with an MOI of 5. At 15h p.i. cells were metabolically labeled for 1h. Cell were lysed by IP lysis buffer with 1% Igepal. Precipitation was performed using anti-gpUS6 antiserum (8µl 7510). PAS was added and incubated for 1h. Precipitated proteins were separated by a 10% SDS-PAGE. The gel was dried and exposed to an autoradiography X-ray film for 24h. The molecular weight marker is shown on the left side.

As can be seen in Fig. 4.4, gpUS6sol migrates with an apparent molecular weight of 16 kDa, compatible with the protein sequence of 139 aa. After Endo H digestion retardation of both wt gpUS6 and gpUS6sol is altered because of removal of the N-glycosylation, proving an ER lumenal localization. Glycoproteins that have passed the trans-golgi network are no longer sensitive to Endo H. Since gpUS6 and gpUS6sol do not exhibit Endo H resistance, this result indicates that wt gpUS6 and gpUS6sol are retained in the ER. Hence, the constructed gpUS6sol-rVV expressed the expected gpUS6 mutant protein which was localized to the ER lumen.

SUMMARY

- **The fraction E2 of the purified anti-gpUS6 antiserum 7510 (1262) precipitates gpUS6 and complexed TAP subunits with minimal background.**
- **The soluble gpUS6 mutant (aa 1-139) is stably expressed and localizes to the ER lumen.**

4.2 gpUS6 species-specificity

4.2.1 Inactivation of TAP by gpUS6 is species-restricted

Herpesviruses are pathogens with a long history of co-speciation with their host leading to a close adaptation of molecular functions. As a consequence, some of the herpesviral inhibitors of the MHC class I pathway, including the herpes simplex virus encoded inhibitor of TAP, ICP47 (Ahn et al., 1996), exhibit a remarkable species-restriction in their target specificity (Tomazin et al., 1998). This has also been shown to be true for gpUS6 in previous experiments in collaboration with Dr. Frank Momburg, DKFZ, Heidelberg.

A starting point for this work was the establishment of the TAP dependent peptide translocation assay by viable cells to confirm the findings of gpUS6 species-specificity. In the peptide translocation assay the ^{125}I-labeled peptides containing an N-glycosylation site are added to permeabilized cells and analyzed for glycosylation. If cells possess a functional TAP complex the addition of ATP leads to peptide transport into the ER lumen where glycosylation takes place. After cell lysis the glycosylated peptides are collected by Con A sepharose and γ-counts retrieved from the Con A sepharose and lysates are determined (for details see Experimental procedures). To determine the background level (negative control) of the assay, peptide transport was measured in the presence of EDTA instead of ATP. When the conditions were set, human Hela and rat Rat-2 cells were infected with rVV expressing gpUS6 or a control gene for measuring of gpUS6 influence on TAP function. As can be seen in Fig. 4.5, transport of peptide was measured in both cell lines infected with the rVV control virus. In human HeLa cells expression of gpUS6 decreased transport of peptide by almost 80% in comparison to HeLa cells infected with the control virus. In contrast, in rat cells peptide translocation was not impaired by gpUS6. The data verify earlier findings, that gpUS6 inhibits TAP in a species dependent manner, and that rat TAP resists functional inactivation by gpUS6.

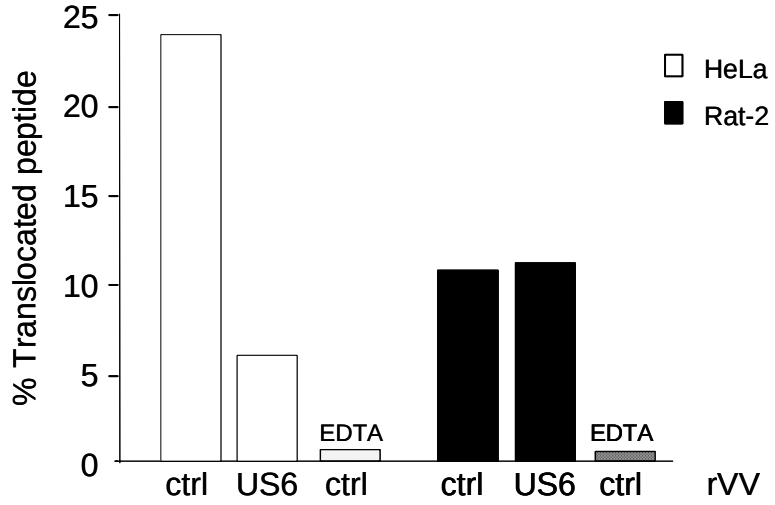

Fig. 4.5 gpUS6-mediated inhibition of peptide transport in human and rat cells.

The indicated cell lines were infected with gpUS6-rVV or with control (ctrl)-rVV (UL118-rVV) at an MOI of 4. At 15h p.i. cells were permeabilized and peptide translocation was assessed as described in Experimental procedures. Transport rates are given as means of duplicate values.

4.2.2 gpUS6 binding to both TAP subunits is required for efficient inactivation of peptide transport

Earlier gpUS6 binding studies in our lab using human and rat TAP1 and TAP2 subunits (hT1, hT2, rT1, rT2) showed that only when human TAP1 and human TAP2 were co-expressed, co-precipitation of both subunits by gpUS6 could be observed. Single expression of human TAP1 or TAP2 subunits did not result in gpUS6 recognition. Co-expressed rat TAP subunits on the contrary, were not precipitated by anti-gpUS6 antibodies. However, when one rat subunit was combined with a human counterpart (hT1 with rT2 or rT1 with hT2) both subunits of heterodimeric complexes were efficiently co-precipitated. From these data the conclusion was drawn that both human TAP1 and TAP2 subunits each contain independent recognition sites for gpUS6. Consequently, gpUS6 binding to a single TAP chain is sufficient for precipitating the preformed heterodimeric TAP complex, the formation of which depends on TAP subunit assembly with a complementary TAP molecule.

In order to analyze the impact of gpUS6 binding to chimeric TAP dimers on a functional level a peptide translocation assay using rVV-expressed TAP subunits was established. The CMT64.5 mouse cell line has a defective promoter for TAP (Klar and Hammerling, 1989), hence, the cell line lacks constitutive TAP gene expression and can not translocate peptides to the lumen of ER. Therefore, conditions for optimal inhibition of peptide translocations by

rVV-expressed TAP subunits were examined in CMT64.5 cells. CMT64.5 and CMT64.5-*US6* cells were infected with hT1-rVV and hT2-rVV only or in combination with a third rVV expressing a TAP inhibitor or a control gene. The rVV expressed TAP subunits reconstituted TAP function in CMT64.5 cells, resulting in translocation of 6% of the input peptide in an ATP dependent manner, whereas non-infected CMT64.5 cells did not translocate the peptide (0,36% versus 0,11% in the EDTA negative control) (Fig. 4.6). Co-infection with a third control rVV did not influence the efficiency of peptide translocation, whereas expression of the characterized TAP inhibitor ICP47 led to an almost complete loss of TAP function. Only 8% residual TAP activity could be measured in the presence of ICP47. With gpUS6 however, TAP inhibition was less effective as with ICP47. Co-expressed gpUS6 by rVV inhibited only 50% of the TAP dependent peptide translocation. Using the soluble mutant of gpUS6 the inhibition was even lower than with wt gpUS6, resulting in 64% residual TAP activity. One may speculate that this is a result of the missing TMS of gpUS6sol, which can not be fixed to the ER membrane and therefore gpUS6sol does not find its target protein as efficiently as the wt gpUS6. The most efficient inhibition by gpUS6 was achieved using the CMT64.5-*US6* cell line. 40% residual TAP activity (60% gpUS6-mediated inhibition) was measured in CMT64.5-*US6* cells in comparison to non-transfected cells. This setting was chosen for further analysis of gpUS6-mediated inhibition of TAP function.

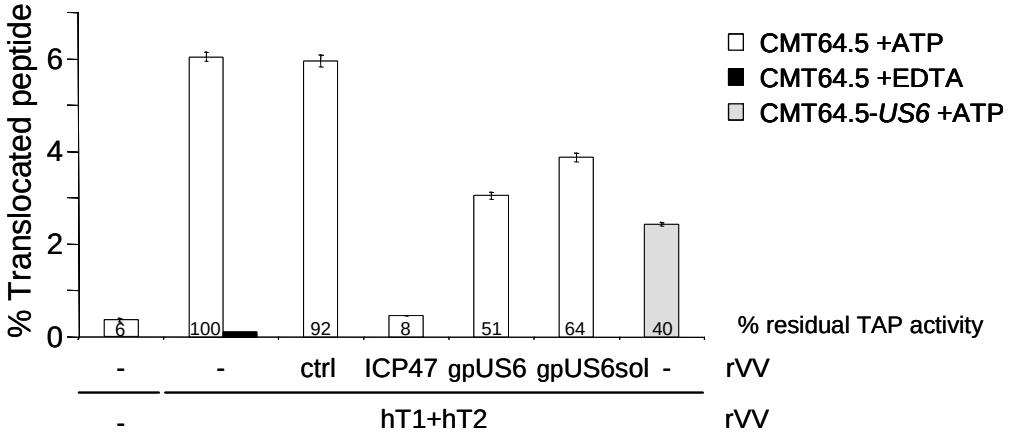

Fig. 4.6 Inhibition of peptide transport by rVV expressed TAP subunits.

CMT64.5 or CMT64.5-*US6* cells were infected with human TAP1 and human TAP2 expressing rVV with an MOI of 5. In addition, a third rVV was co-infected as indicated (ctrl-rVV was UL118-rVV). At 10h p.i. cells were permeabilized and peptide translocation was assessed as described in Experimental procedures. Residual TAP activity is given as the percentage peptide transport of the peptide transport by rVV expressed hT1+hT2 without co-expression by a third rVV (second bar in diagram).

The question whether gpUS6 binding to a single TAP subunit is sufficient for inhibition of peptide translocation could now be approached. Peptide translocation was assessed as described above. CMT64.5 and CMT64.5-*US6* cells were infected with combinations of rVVs expressing human and rat TAP1 and TAP2. In this setting, again peptide translocation was inhibited by about 60% in *US6*-transfected cells when compared to non-transfected CMT64.5 cells after reconstitution with human TAP (Fig. 4.7). As expected, peptide translocation by rat TAP subunits was not inhibited in the CMT64.5-*US6* cell line. After expression of combinations of human/rat transporter subunits, i.e. hT1/rT2 or rT1/hT2, gpUS6 inhibition reached about half of the inhibition rate of hT1/hT2. Thus, gpUS6 binding to both subunits is a prerequisite for efficient functional inactivation of peptide translocation.

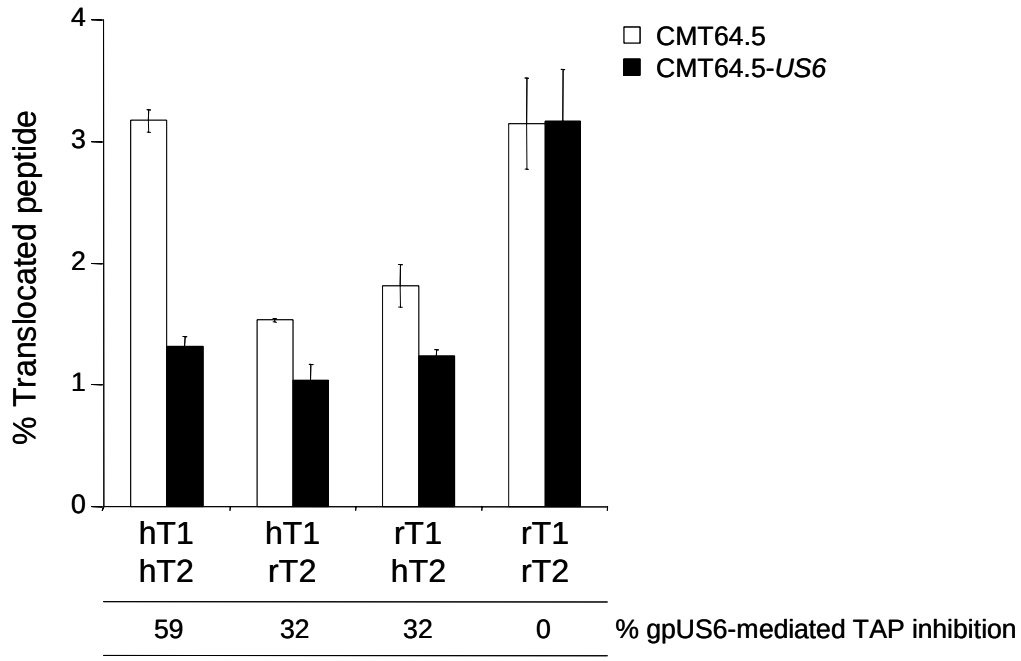

Fig. 4.7 gpUS6-mediated inhibition of rVV expressed human and rat TAP subunits.

Non-transfected or *US6*-transfected CMT64.5 cells were infected with rVV expressing TAP1 and TAP2 subunits as indicated at an MOI of 4. At 10h p.i. cells were permeabilized and peptide translocation was assessed as described in Experimental procedures. gpUS6-mediated inhibition is expressed as the percentage of the difference of transport values in *US6*-transfected cells in comparison to non-transfected cells.

SUMMARY

- **Peptide translocation by endogenously expressed TAP in human HeLa but not in rat Rat-2 cells is inhibited by gpUS6, i.e. gpUS6 is species-restricted.**
- **Efficient inhibition of peptide translocation by TAP requires gpUS6 binding to both TAP subunits.**
- **gpUS6 interaction with combinations of human/rat TAP subunits mediates only half of the maximal inhibition rate.**

4.3 Probing the TAP1 TMD by gpUS6

4.3.1 The TAP1 C-terminal TMD contains a binding site for gpUS6

gpUS6 species-restriction is remarkable, when considering the high degree of homology of human and rat TAP protein sequences, which is about 80%. These features, the species-specificity of gpUS6 and the close identity of human and rat TAP, offered an expedient approach for localization of gpUS6 binding domains on TAP. Based on conserved restriction enzyme sites, intrachain human/rat TAP1 chimeras were constructed. Since the gpUS6 ectodomain has been shown to suffice for TAP inhibition (Ahn et al., 1997; Hewitt et al., 2001; Kyritsis et al., 2001), it was supposed that the gpUS6 interaction domain on TAP is localized within the transmembrane domain (TMD) and not to the cytosolic nucleotide binding domain (NBD). Therefore, the TMD of TAP1 was selected for sequence substitution. The first set of TAP1 chimeras constructed and analyzed is depicted in Fig. 4.8.

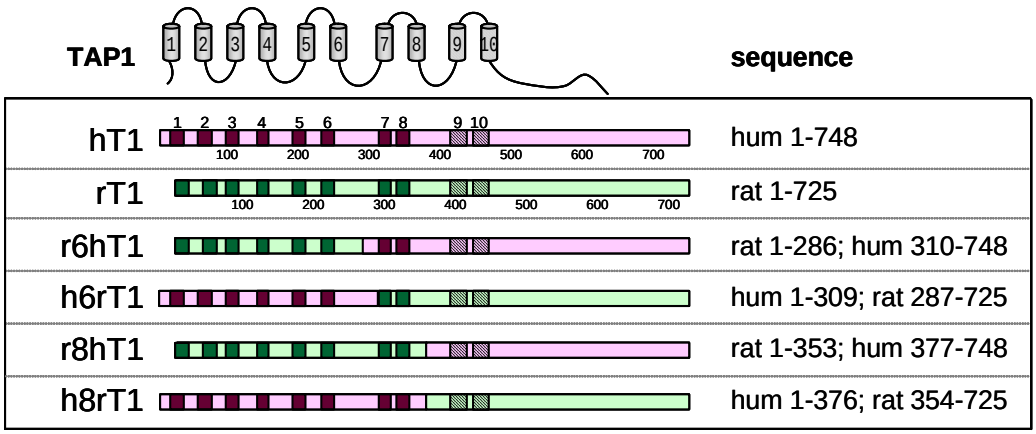

Fig. 4.8 Schematic representation of intrachain human/rat TAP1 chimeras.

Human sequences are shown in red and rat sequences in green. Boxes indicate predicted TMSs (Abele and Tampe, 1999) numbered from 1-10 and the controversial TMS9 and 10 are striped.

A first analysis for verification of correct formation and function of the chimeric TAP subunits was carried out. Peptide transport was measured for each rVV expressed chimera in complex with both human and rat TAP2. All TAP1 chimeric subunits showed satisfying transport rates even if the transport efficiencies varied (Fig. 4.9). The chimeras r6hT1 and r8hT1 transported peptide at comparable levels with both a human and a rat TAP2 counterpart. Efficiency of peptide transport by h6rT1 and h8rT1, on the other hand, appeared to be dependent on the species of the TAP2 subunit. In complex with human TAP2 the

transport was less efficient than with rat TAP2. Especially for h6rT1 the difference was pronounced, indicating that species-dependent interactions between TAP1 and TAP2 may take place. This was also observed for the wt subunits. However, the functionality of all TAP1 chimeras was verified and further analysis could be proceeded.

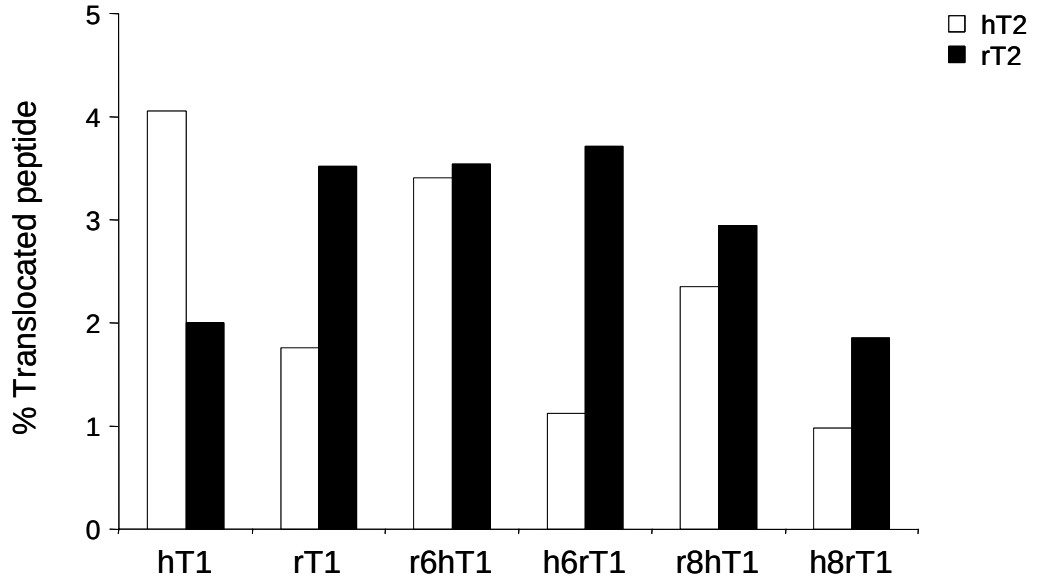

Fig. 4.9 Peptide translocation by rVV expressed TAP1 chimeras.

TAP deficient CMT64.5 cells were infected with an MOI of 4 with rVV expressing TAP subunits as indicated. At 10h p.i. peptide translocation was measured as described in Experimental procedures. Diagram shows per cent peptide translocation by TAP1 chimeras co-expressed with hT2, open bars, or with rT2, filled bars. Transport rates are given as means of duplicate values.

Binding of gpUS6 to TAP1 chimeras was analyzed by co-IP. Apparent complex formation between the TAP1 chimeras and wt human TAP2 was indicated by the presence of TAP1 subunits in gpUS6 precipitates (data shown only for h6rT1 and h8rT1, Fig. 4.10, lanes 5 and 7), since gpUS6 binds to preformed TAP1/2 heterodimers only. To define domains on TAP1 sufficient for gpUS6 interaction, the TAP1 chimeras were combined with the rat TAP2 subunit. Since rat TAP2 lacks recognition sites for gpUS6 only TAP1 chimeras containing a gpUS6 recognition site can be precipitated by gpUS6. While in the presence of the r6hT1 chimera anti-gpUS6 antibodies co-precipitated rTAP2, this was not the case for the h6rT1 chimera and rTAP2 (Fig. 4.10, lane 6 and 11). Both the r8hT1 and the h8rT1 chimera were precipitated in combination with rTAP2. This result suggests that the chimera h6rT1 does not possess any recognition sites for gpUS6, whereas two independent domains for gpUS6 binding are formed by the chimeras r8hT1 and h8rT1.

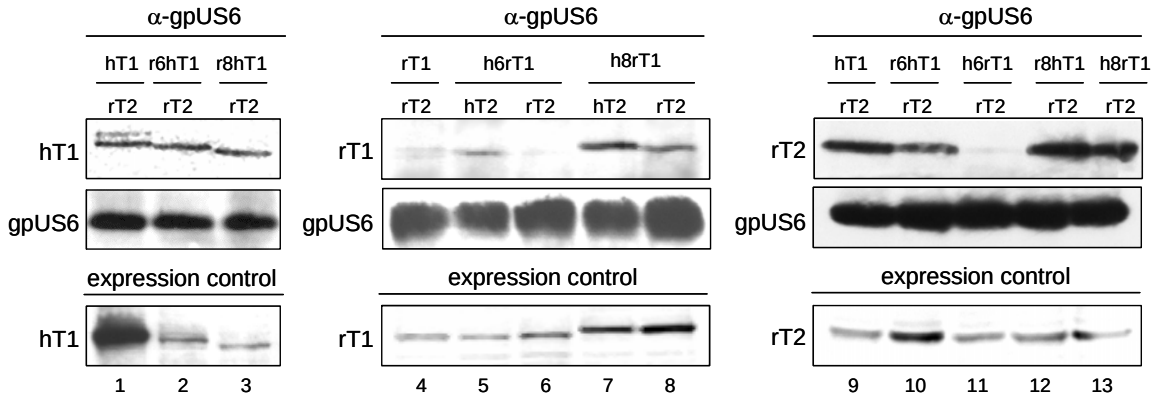

Fig. 4.10 Co-precipitation of gpUS6-associated TAP1 chimeras.

TAP subunits were expressed by rVV in *US6*-transfected CMT64.5 cells. At 15h p.i. digitonin lysates were prepared and gpUS6-TAP complexes were immunoprecipitated by rabbit anti-gpUS6 antiserum (12µl 7510). Proteins were separated by 10% SDS-PAGE, before transferred to a nitrocellulose membrane. The membrane was cut in two parts, one above the 50 kDa marker band for detection of TAP subunits and one below for detection of gpUS6. Human TAP1 subunits were detected by 148.3, rat TAP1 by D90, rat TAP2 by D116 and gpUS6 by 7510 antiserum. For control of expression, an aliquot of each lysate was analyzed by Western blot.

To test the functional influence of gpUS6 interaction with the human/rat TAP1 chimeras peptide translocation efficiency was determined in CMT64.5 in comparison to CMT64.5-*US6* cells. The degree of gpUS6-mediated inhibition of the TAP1 chimeras combined either with hTAP2 or with rTAP2 is shown in Fig. 4.11. The chimeras r6hT1 and r8hT1 behaved like hT1, i.e. when combined with hT2 their peptide translocation capacity was inhibited by 50-60% by gpUS6. When combined with rTAP2 the gpUS6-mediated inhibition reached only about 25-30%. In contrast, the chimeras h6rT1 and h8rT1 showed results comparable to rTAP1. When combined with rTAP2 the gpUS6-mediated inhibition was lost, and the combination with hTAP2 yielded an inhibition of about 20%. From these results it was concluded that a human sequence in the last C-terminal TMD of TAP1 is necessary and sufficient to mediate binding and inhibition by gpUS6. A surprising result, since this part of the TAP1 TMD has been subjected to controversial discussions regarding its membrane topology. The findings presented here point at a loop localized in the lumen at some point downstream of aa 377 of TAP1. The second gpUS6 binding domain found on the chimera h8rT1 did not mediate significant inhibition of peptide translocation.

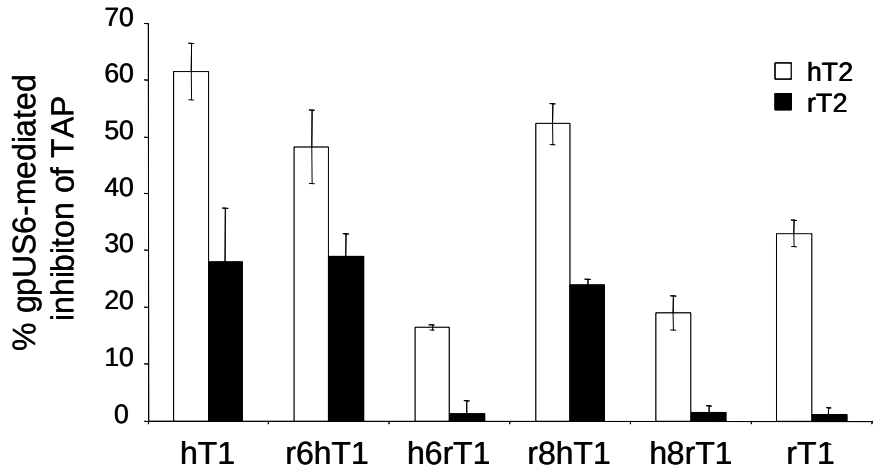

Fig. 4.11 gpUS6-mediated inhibition of peptide translocation by rVV expressed TAP1 chimeras.

TAP deficient CMT64.5 cells, non-transfected or *US6*-transfected, were infected at an MOI of 4 with rVV expressing TAP subunits as indicated. At 10h p.i. peptide translocation was measured as described in Experimental procedures. gpUS6-mediated inhibition of TAP1 chimeras co-expressed with hT2 is shown as open bars and with rT2 as filled bars. gpUS6-mediated inhibition is expressed as the percentage of the difference of transport values in *US6*-transfected cells in comparison to non-transfected cells.

4.3.2 A soluble gpUS6 recognizes r8hT1, implying a TAP1 topology with 10 TMS

Previous work has shown that a C-terminal truncated gpUS6 mutant, lacking the TMS and the cytosolic tail, maintains the ability to inactivate TAP (Ahn et al., 1997; Hewitt et al., 2001; Kyritsis et al., 2001), implying a strictly lumenal TAP-gpUS6 interaction. We therefore hypothesized that human sequences of the r8hT1 chimera required for gpUS6 recognition should be able to traverse the ER membrane and form the gpUS6 binding site in the ER lumen, which would indicate that TAP1 molecules indeed form the controversial fifth pair of TMSs. To corroborate this assumption a further TAP1 chimera was constructed, lacking all human sequences which might be part of the TMD (rxhT1, Fig. 4.12).

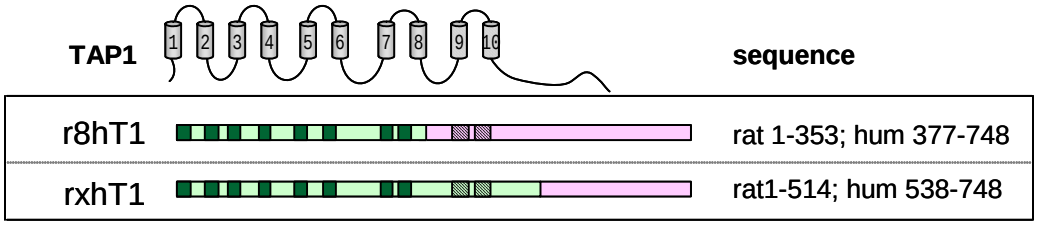

Fig. 4.12 Schematic representation of intrachain human/rat TAP1 chimeras r8hT1 and rxhT1.

Human sequences are shown in red and rat sequences in green. Boxes indicate predicted TMSs (Abele and Tampe, 1999) numbered from 1-10 and the controversial TMS9 and 10 are striped.

The chimeras were co-expressed by rVV together with rat TAP2 in CMT64.5-*US6* cells. Digitonin lysates were prepared and gpUS6 binding was analyzed by co-IP using anti-gpUS6 antibodies. In order to assess the magnitude of gpUS6 recognition the precipitated material was loaded to the gel in three steps of dilution. Comparison of gpUS6 binding to the r8hT1 and the rxhT1 chimera revealed a clear difference. Displayed in Fig. 4.13, for equal band intensity the r8hT1/rT2-sample co-precipitated by gpUS6 was more than fourfold higher diluted than the precipitated rxhT1/rT2-sample. The binding assay indicates that the rxhT1 mutant lacks a binding site for gpUS6. To ensure an exclusively lumenal interaction between gpUS6 and r8hT1, binding by the soluble truncated mutant of gpUS6 (aa 1-139) was analyzed. gpUS6sol selectively recognized r8hT1 but not rxhT1, confirming that the ER lumen is the site of gpUS6-TAP1 interaction. The peptide translocation assay brought further evidence that the rxhT1 chimera is not recognized by gpUS6, since rxhT1 is behaving rT1-like (Fig. 4.14). Thus, TAP1 recognition by gpUS6 requires the presence of human sequences in the C-terminal part of the TMD between aa 377 and 537, which are exposed to the ER lumen. This finding suggests that the controversial TMS9-10 in the core TMD must exist.

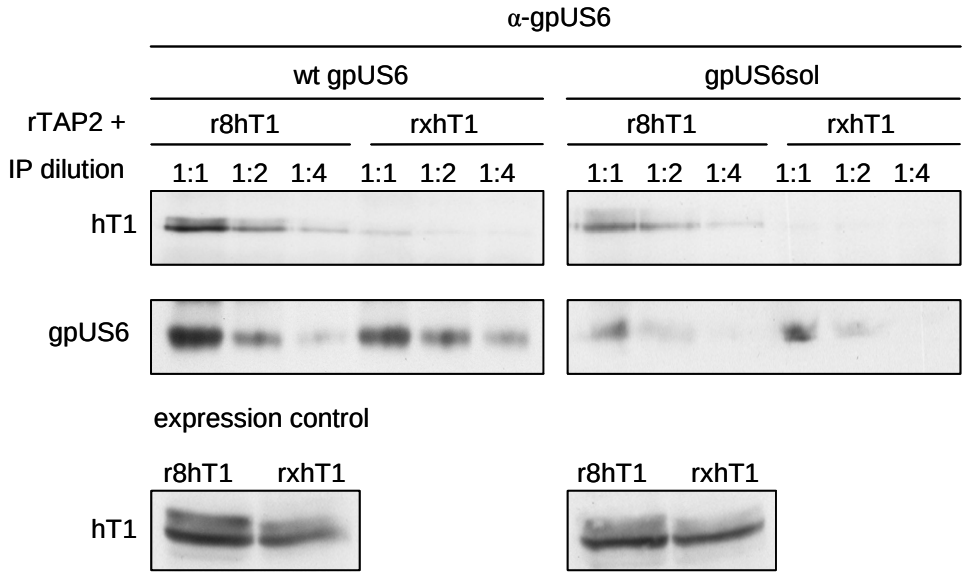

Fig. 4.13 Co-precipitation of r8hT1 and rxhT1 by wt and soluble gpUS6.

TAP subunits, wt gpUS6 and gpUS6sol were expressed by rVV in CMT64.5 cells as indicated. At 15h p.i. digitonin lysates were prepared and gpUS6-TAP complexes were immunoprecipitated by rabbit anti-gpUS6 antiserum (12µl 7510). Precipitated proteins were diluted in three log2 steps for quantification of TAP-gpUS6 interaction. Proteins were separated by 10% SDS-PAGE and transferred to a nitrocellulose membrane for detection by Western blotting. The membrane was cut in two parts, one above the 50 kDa marker band for detection of hT1 by 148.3 and one below for detection of gpUS6 by 7510 antiserum. For control of expression, an aliquot of each lysate was analyzed by Western blot.

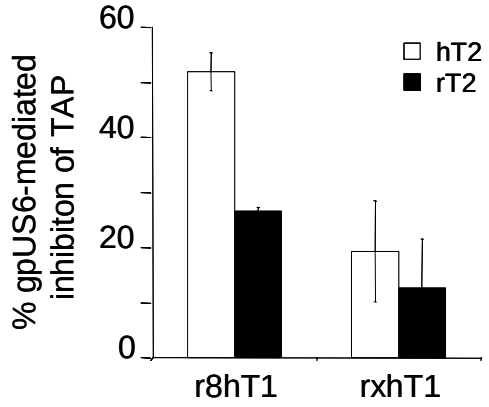

Fig. 4.14 gpUS6-mediated inhibition of peptide translocation by r8hT1 and rxhT1.

TAP deficient CMT64.5 cells, non-transfected or *US6*-transfected, were infected at an MOI of 4 with rVV expressing TAP subunits as indicated. At 10h p.i. peptide translocation was determined as described in Fig. 4.11.

4.3.3 The predicted fifth lumenal loop of TAP1 is not responsible for the inhibitory effect of gpUS6

Based on sequence alignment with the MDR (multidrug resistance) transporter P-gp a putative membrane topology for TAP was proposed (Abele and Tampe, 1999). Furthermore, the accuracy of the alignment with P-gp was supported by the sequence comparison with the MsbA transporter (see Appendix I), which has been experimentally confirmed for the first time by the findings above. Accordingly, the r8hT1 chimera exposes a putative loop comprising 9 aa of the human sequence within the ER lumen, forming the fifth C-terminal lumenal loop of TAP1 between TMS9 and TMS10. This sequence is shared between human and rat TAP1 except for replacement of threonine (T) and a serine (S) at positions 435 and 436, respectively, in the human sequence by valine (V) and arginine (R) at positions 412 and 413 in the rat sequence (see sequence alignment in Fig. 4.15). Substitution of TS for VR in the r8hT1 chimera (r8hVRT1) was performed to analyze the role of loop 5 for gpUS6 recognition.

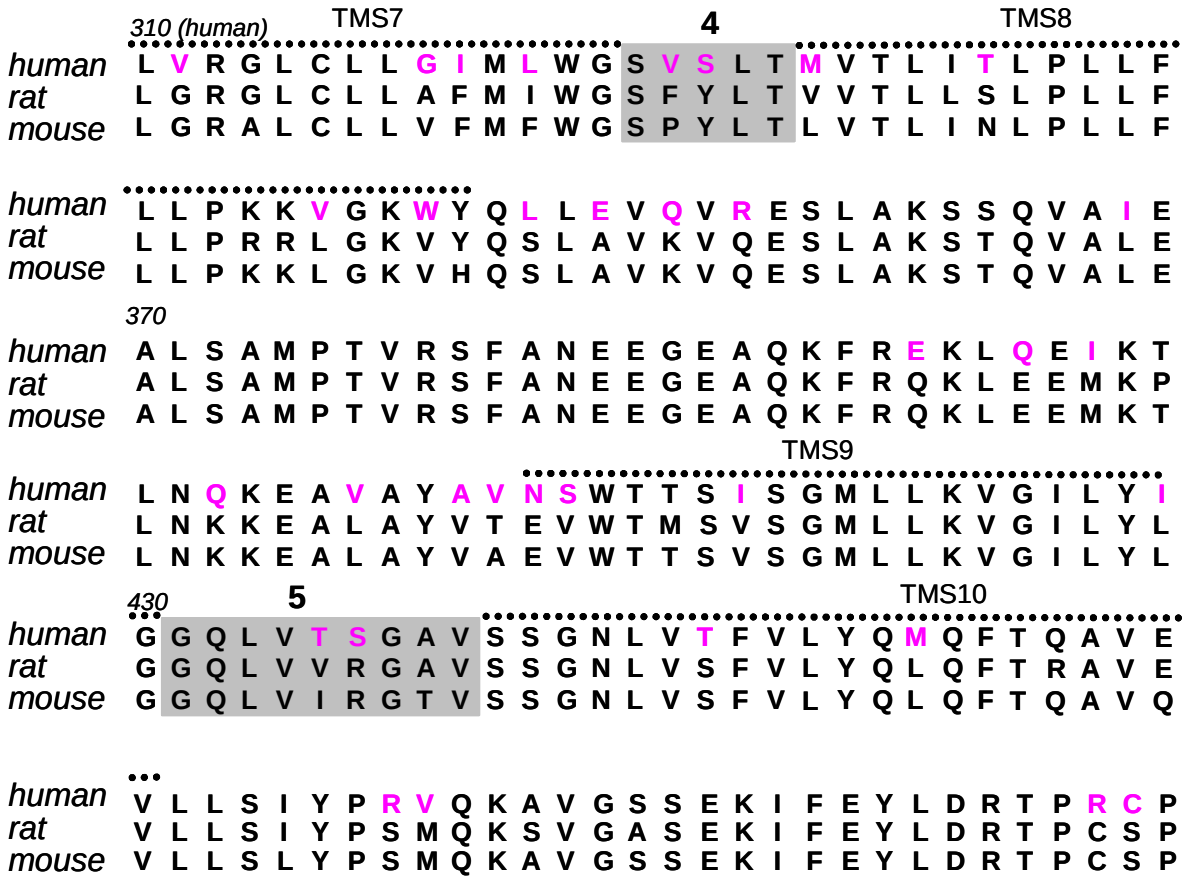

Fig. 4.15 Sequence alignment of the TMS7-10 of human, rat and mouse TAP1.

Human amino acids differing from both rat and mouse sequences are highlighted in red. Putative TMS7-10 (Abele and Tampe, 1999) are marked with a dotted line and putative lumenal loops 4-5 are indicated by grey boxes.

As demonstrated in Fig. 4.16, gpUS6 bound to both TAP1 chimeras and inhibited peptide transport with similar efficiency, indicating that there was no significant difference of gpUS6 interaction with the chimeras r8hT1 and r8hVRT1. The findings imply that the hTAP1 aa 431-439 that constitute the predicted fifth lumenal loop are not sufficient for recognition and binding by gpUS6.

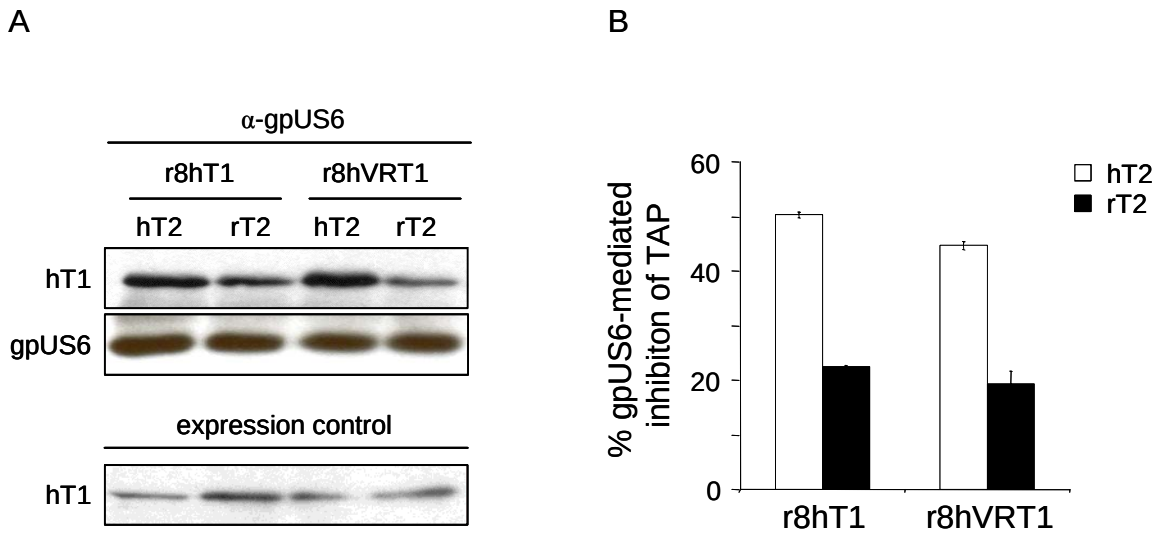

Fig. 4.16 Substitution of TS by VR in the fifth predicted loop does not prevent gpUS6 recognition and inhibition of TAP1.

A. gpUS6 binding to r8hVRT1 was assessed by co-IP as described in Fig. 4.10. B. Peptide translocation assay was performed as described in Fig. 4.11.

SUMMARY

- **gpUS6 recognizes two independent domains on TAP1, but only one is required for efficient inhibition: aa 376-537 mediate binding and inhibition, aa 310-376 mediate binding but no inhibition.**
- **The C-terminal binding domain is recognized by a soluble gpUS6, indiacting a lumenal localization for the binding site, i.e. TAP1 traverses the ER membrane C-terminal of residue 376 and forms TMS9-10.**
- **The predicted fifth lumenal loop formed between TMS9-10 does not confer the gpUS6-mediated inhibition of peptide translocation.**

4.4 gpUS6 interaction with TAP2

gpUS6 recognizes domains formed on both subunits of the heterodimeric TAP complex. Binding to one is sufficient for co-precipitation of the complex, whereas efficient functional inhibition requires gpUS6 interaction with both TAP1 and TAP2. Since the TAP1 intrachain human/rat chimeras proved to be functional and suitable for the interaction analysis with gpUS6, a set of TAP2 intrachain human/rat subunits was constructed (Fig. 4.17).

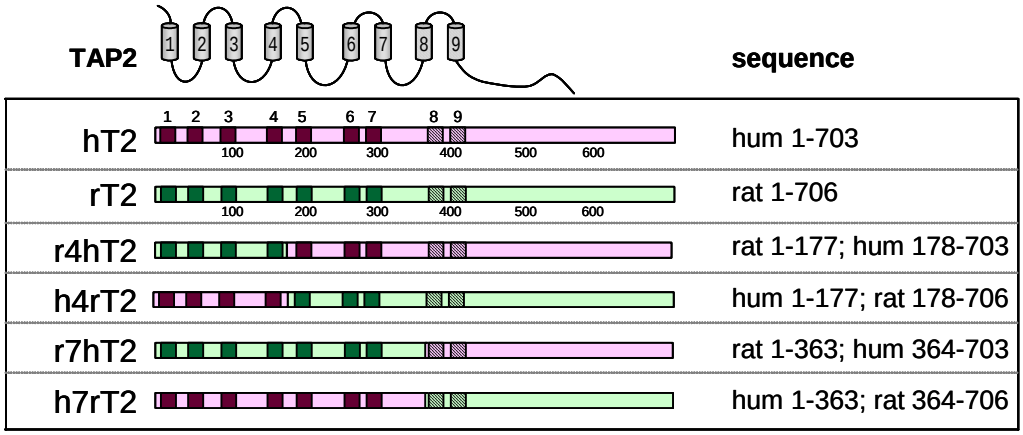

Fig. 4.17 Schematic representation of intrachain human/rat TAP2 chimeras.

Human sequences are shown in red and rat sequences in green. Boxes indicate predicted TMSs (Abele and Tampe, 1999) numbered from 1-9 and the controversial TMS8 and 9 are striped.

First, the functionality of the TAP2 chimeras was tested in CMT64.5 cells infected by rVV expressing the TAP2 subunits together with either a human or rat TAP1 counterpart. Like the TAP1 chimeras, all chimeric TAP2 constructs were functional although differing transport rates could be observed (Fig. 4.18). The most striking chimera was the h4rT2 which transported the peptide very effectively with human TAP1 and even stronger with rat TAP1.

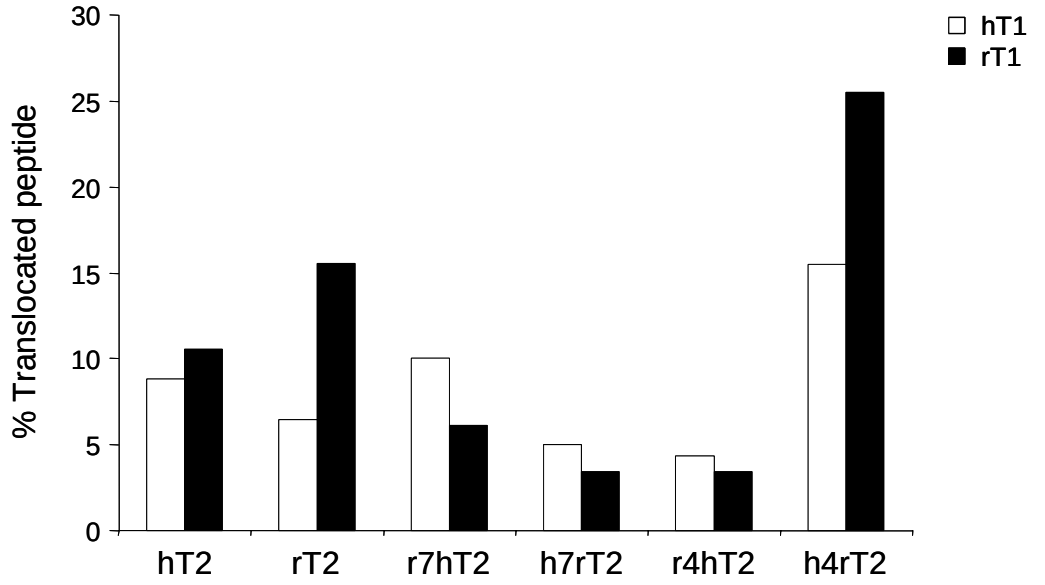

Fig. 4.18 Peptide translocation by rVV expressed TAP2 chimeras.

TAP deficient CMT64.5 cells were infected with an MOI of 4 with rVV expressing TAP subunits as indicated. At 10h p.i. peptide translocation was measured as described in Experimental procedures. Diagram shows per cent translocation of TAP2 chimeras co-expressed with hT1, open bars, or with rT1, filled bars. Transport rates are given as means of duplicate values.

4.4.1 Inhibition of TAP2 by gpUS6 is directed by the C-terminal TMD

Next, gpUS6-mediated inhibition of peptide translocation by the TAP2 chimeras was assessed (Fig. 4.19). The chimeras r4hT1 and h7rT1 were most efficiently inhibited by gpUS6, reaching 40-45% inhibition in combination with hT1, which is still less efficient than the wt combination hT1/hT2 (60%), indicating that these chimeras might lack a further interaction site (or sites) for gpUS6. Transport function of chimeras h4rT2 and h7rT2 was almost not affected by gpUS6. As a result, the inhibitory effect of gpUS6 on TAP2 is found to follow a similar pattern as for TAP1, i.e. inhibition is forwarded by the C-terminal TMD.

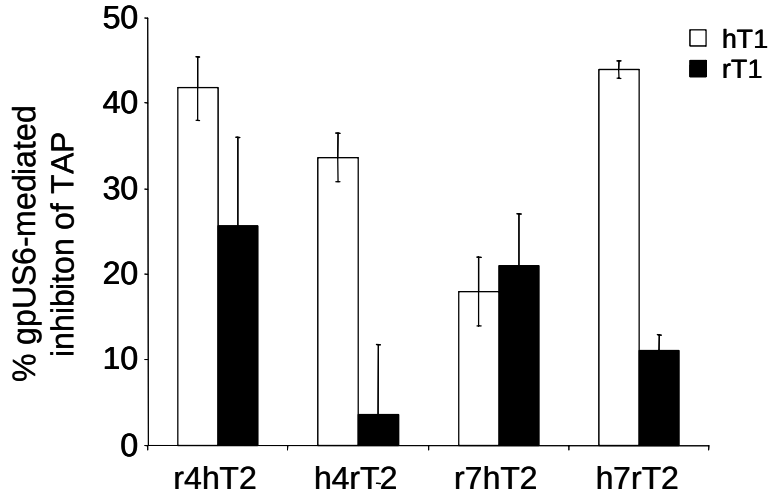

Fig. 4.19 gpUS6-mediated inhibition of TAP2 chimeras.

TAP2 chimeras were expressed by rVV together with hT1 or rT1 in *US6*-transfected or non-transfected CMT64.5 cells. At 10h p.i. peptide translocation was measured as described in Experimental procedures. gpUS6-mediated inhibition of TAP1 chimeras co-expressed with hT1 is shown as open bars and with rT1 as filled bars. gpUS6-mediated inhibition is expressed as the percentage of the difference of transport values in *US6*-transfected cells in comparison to non-transfected cells.

4.4.2 The gpUS6 binding domain on TAP2 localizes to the N-terminal TMD

For mapping of the domain responsible for gpUS6 binding, the human/rat TAP2 chimeras were co-expressed with the rat TAP1 subunit. The result is depicted in Fig. 4.20. In contrast to the TAP1 subunit, gpUS6 binding to TAP2 was mapped to the N-terminal TMD, to residues 1-177. The chimeras h7rT2 and h4rT2, when combined with rT1, were recognized by gpUS6 (Fig. 4.20, lanes 5 and 9), while r7hT2 and r4hT2 were not (Fig. 4.20, lanes 3 and 7). The same binding pattern of TAP2 chimeras was found after expression of gpUS6sol (Fig. 4.21). Surprisingly, the determined binding domain for gpUS6 on TAP2 is distinct from the domain crucial for inhibition of peptide translocation. This finding points at a different mode of interaction of gpUS6 with TAP2 than with TAP1.

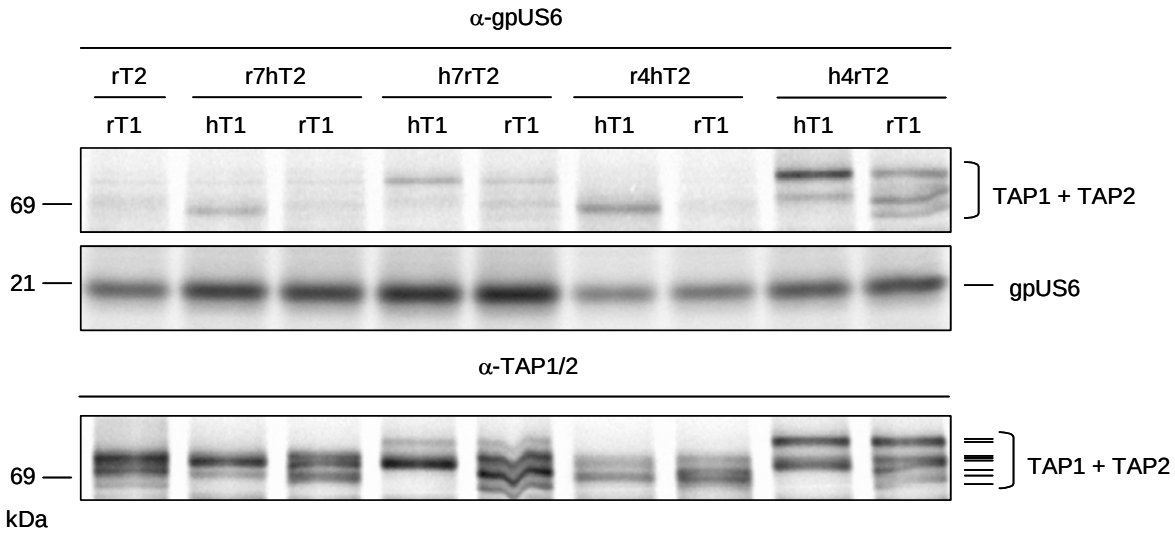

Fig. 4.20 Analysis of gpUS6 binding to TAP2 chimeras.

Combinations of TAP2 chimeras with hT1 or rT1 were co-expressed by rVV in *US6*-transfected CMT64.5 cells as indicated. Binding of gpUS6 to TAP was assessed in metabolically labeled cells by co-IP using 12µl E2 (7510). Expression of TAP subunits was controlled by anti-TAP antibodies: hT1 and rT1 were precipitated by TAP1.28 (2µl) and RatTAP1 (1,7µl), respectively, r7hT2 and r4hT2 by TAP2.17 (2µl) and h7rT2 and h4rT2 by RatTAP2 (2,1µl)). Immunocomplexes were collected by PAS (PGS for RatTAP1 and 2 antiserum). Precipitated proteins were separated by a 10-13% gradient SDS-PAGE. The gel was dried and exposed to an autoradiography X-ray film for 24h. The molecular weight marker is shown on the left side. TAP subunits are indicated by lines to the right, beginning from the top (rT1 comes as two bands, rT1a and rT1b): h4rT2, h7rT2, rT2, rT1a, hT1, r7hT2, r4hT2, rT1b.

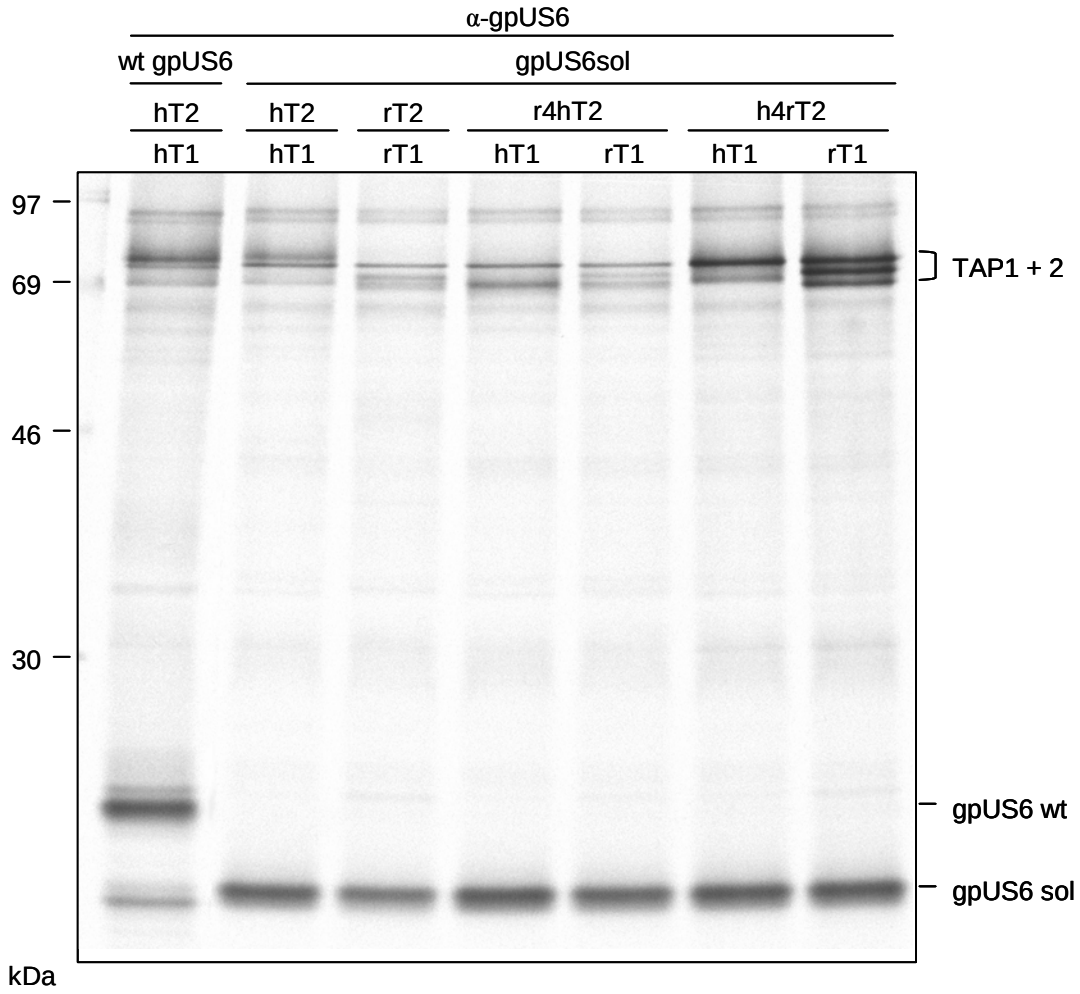

Fig. 4.21 Analysis of gpUS6sol binding to TAP2 chimeras.

Combinations of TAP2 chimeras with hT1 or rT1 were co-expressed by rVV together with gpUS6sol-rVV or gpUS6-rVV in CMT64.5 cells as indicated. Binding of gpUS6sol to TAP was assessed in metabolically labeled cells by co-IP using anti-gpUS6 antibodies as described in Fig. 4.20.

SUMMARY

- **Efficient inhibition of TAP2 is mediated by residues C-terminal of aa 178, but no gpUS6 binding to this part of TAP2 is observed.**
- **Stable lumenal gpUS6 binding to TAP2 is located N-terminal of aa 177.**
- **gpUS6 interaction with TAP1 and TAP2 does not follow a similar pattern.**

4.5 Oligomerization of gpUS6

Based on the findings above, 4 gpUS6 interaction sites on TAP evidently exist, two of which are located to TAP1 and two to TAP2. This raised the question whether the ectodomain of gpUS6 might be able to access all interaction sites at the same time. Noticing the fact that the sequence of gpUS6 contains 8 cysteines (Fig. 4.1), it was investigated whether gpUS6 might form homodimers to bridge the recognition sites between the TAP heterodimer. For analysis of intermolecular disulfide bridges gpUS6 was expressed in CMT64.5 cells by rVV. Cells were lysed in IP-lysis buffer and proteins were separated by SDS-PAGE in parallel under reducing or non-reducing conditions followed by Western blotting using gpUS6-specific antibodies. ICP47 expressing rVV was used as a negative control. The result depicted in Fig. 4.22 shows under non-reducing conditions a prominent band just above the 38 kDa marker band, which fits with the molecular weight of 42 kDa for the gpUS6 homodimer. Moreover, multiple further bands exhibiting a molecular weight of n x 21 kDa were detected under non-reducing conditions, which contracted to a single 21 kDa band under reducing conditions corresponding to gpUS6 monomers. The experiment was also performed in lysis buffer containing 1,5mM IAA to prevent the formation of disulfide bridges after cell lysis. Still, there was no alteration in the pattern of gpUS6 oligomerization under non-reducing SDS-PAGE conditions (data not shown). This result indicates that the majority of gpUS6 molecules assembles into homodimers and multimers and thus, is able to reach distant binding sites on TAP.

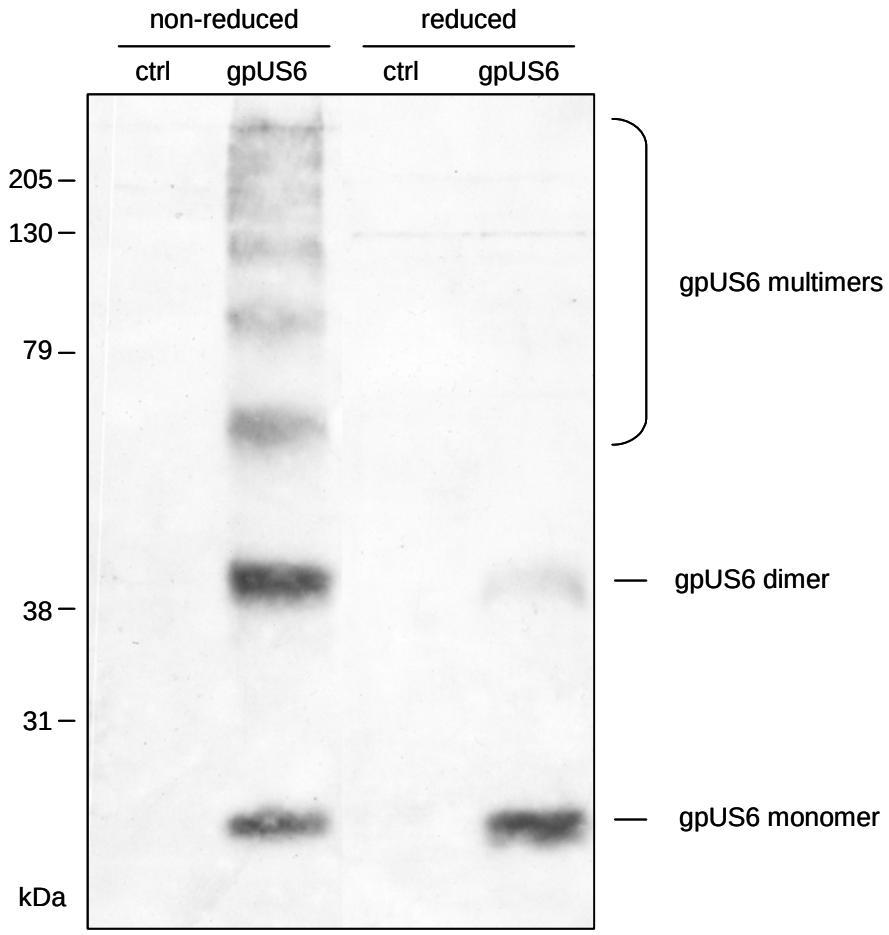

Fig. 4.22 Oligomerization of gpUS6.

gpUS6 was expressed by rVV in CMT64.5 cells. ICP47-rVV was used as a negative control. At 15h p.i. lysates were prepared (IP-lysisbuffer, 1% digitonin) and proteins were separated by 8% SDS-PAGE under reducing or non-reducing conditions. Proteins were detected by Western blot using anti-gpUS6 antibodies (7510).

SUMMARY

- **gpUS6 forms intermolecular di-sulfide bridges resulting in homodimers and multimers.**
- **gpUS6 multimers might facilitate bridging of distant gpUS6 binding domains on TAP.**

4.6 Analysis of Walker A TAP mutants for gpUS6 recognition of the TAP TMD

It has been implied that ATP binding and hydrolysis by the Walker A domains of TAP1 and TAP2 induce conformational changes of TAP. gpUS6, a lumenal inhibitor of TAP (Ahn et al., 1997; Hewitt et al., 2001; Kyritsis et al., 2001), was demonstrated to prevent ATP binding to TAP1 (Hewitt et al., 2001) and thus, considered as a possible sensor for conformational changes transmitted from the NBDs to the lumenal parts of TAP. To investigate the consequences of ATP hydrolysis for gpUS6 recognition of TAP, three different mutants for each TAP subunit were used (Table 4.1). The highly conserved Walker A domain was mutated in TAP1 and TAP2 as follows: (i) the key lysine (K) was substituted for alanine (A) (T1K544A and T2K509A, respectively), (ii) the 9 aa long Walker A domain was deleted (T1Del, T2Del), and (iii) the Walker A domain was replaced by a linker peptide (T1Rep, T2Rep) (Saveanu et al., 2001).

TABLE 4.1
Walker A TAP mutants

TAP	Sequence
T1 T2 wild type	G P N G S G **K** S T
K544AT1 K509AT2 substitution	G P N G S G A S T
DelT1 DelT2 deletion	– – – – – – – – –
RepT1 RepT2 replacement	T H A S S A H A T A S A S A Q A

4.6.1 ATP binding to TAP2 induces conformational changes of the lumenal TMD recognized by gpUS6

Single expressed TAP subunits are not recognized by gpUS6. Therefore, all TAP mutants were expressed together with a wild type human TAP counterpart. Wild type TAP subunits and Walker A TAP mutants and gpUS6 were expressed by rVV in the TAP-deficient *US6*-transfected mouse cell line CMT64.5. Binding of gpUS6 to TAP complexes was assessed by co-IP using anti-gpUS6 antibodies in digitonin cell lysates and precipitated proteins were detected by Western blot. As shown in Fig. 4.23A I and II, lane 1, wt TAP1 and TAP2

subunits were co-precipitated by gpUS6. However, there was a complete loss of gpUS6-binding to TAP complexes containing TAP2 subunits with mutations in the Walker A domain (Fig. 4.23A I and II, lane 2-4). Stability of the TAP2 mutants was shown by the expression control and correct dimerization with wt TAP1 was verified by co-IP with anti-TAP1 antibodies followed by detection of TAP2 by Western blot (Fig.4.23A IV). In contrast, when TAP1 Walker A mutants were co-expressed with wt TAP2, co-precipitation of the TAP complex by gpUS6 antibodies was retained (Fig. 4.23B I). The K544AT1/T2 combination (lane 2) was efficiently bound by gpUS6. K544AT1 even appeared to be stronger co-precipitated by gpUS6 than wt TAP1 (compare expression control, III, and co-precipitation, I). However, RepT1/T2 (lane 4) was recognized to a lesser extent by gpUS6. DelT1 (lane 3) was not stably expressed and therefore not co-precipitated. These observations suggest that ATP binding to TAP2 induces conformational changes required for gpUS6 recognition of TAP, whereas binding and hydrolysis of ATP by TAP1 is not relevant for gpUS6 association with the TAP TMD.

To ascertain that mutations in the TAP2 Walker A domain influenced gpUS6 binding in the ER lumen and not through possible transmembrane or cytosolic interactions, a binding assay with gpUS6sol was performed. gpUS6sol was expressed by rVV together with T1, K544AT1 or RepT1 in combination with T2 and interaction was analyzed by co-IP using anti-gpUS6 antibodies. The ability of gpUS6sol to recognize all TAP combinations demonstrates a lumenal gpUS6 interaction with TAP (Fig. 4.24). Co-IP of TAP complexes by gpUS6sol was weaker than with wt gpUS6, which can be explained by the loss of membrane fixation of gpUS6sol. Taken together, the data presented here provide evidence for conformational changes on the lumenal side of TAP upon ATP binding to TAP2.

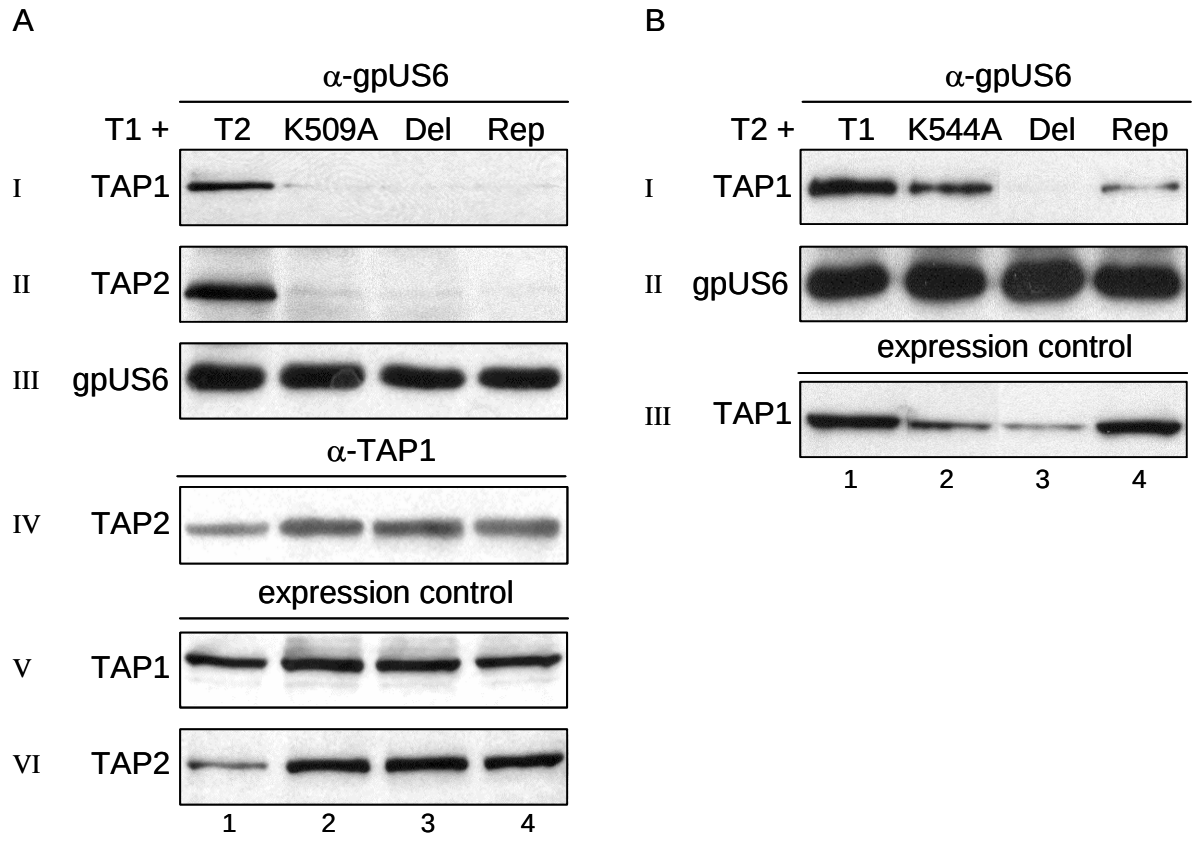

Fig. 4.23 gpUS6 co-precipitation of Walker A TAP mutants.

TAP subunits and gpUS6 were expressed by rVV in *US6*-transfected CMT64.5 cells as indicated. At 15h p.i. digitonin lysates were prepared and gpUS6-TAP complexes were immunoprecipitated by rabbit anti-gpUS6 antiserum (12µl 7510). For TAP1/TAP2 dimerization control, TAP complexes were precipitated by anti-TAP1 antiserum (12µl 7507). After collection of immunocomplexes by PAS, proteins were separated by 10% SDS-PAGE and transferred to a nitrocellulose membrane for detection by Western blot. The membrane was cut in two parts, one above the 50 kDa marker band for detection of T1 and T2 by 148.3 and 439.3, respectively, and one below for detection of gpUS6 by 7510 antiserum. For control of expression, an aliquot of lysates was analyzed by Western blot.

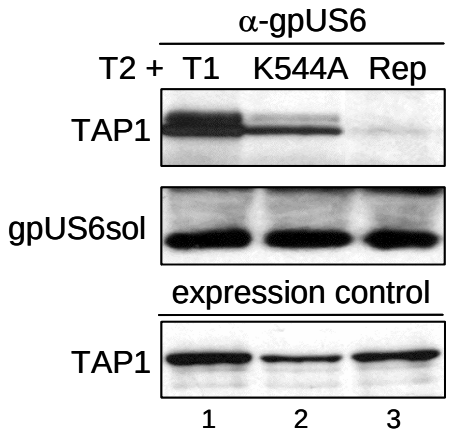

Fig. 4.24 gpUS6sol co-precipitation of Walker A TAP1 mutants.

TAP subunits and gpUS6sol were expressed in CMT64.5 cells by rVV as indicated. At 15h p.i. digitonin lysates were prepared and gpUS6sol-TAP complexes were immunoprecipitated and detected by Western blot as in Fig. 4.23.

4.6.2 gpUS6 binding to TAP1 inhibits binding of ATP to the TAP1 NBD

In a previous study it was shown that ATP binding to TAP1 is inhibited by gpUS6 binding to TAP (Hewitt et al., 2001). Noticing here that ATP binding to TAP2 is required for gpUS6 interaction with TAP, whereas impaired binding of ATP to TAP1 suggested an even more efficient gpUS6-TAP interaction, it was assumed that gpUS6 binding to the TAP1 TMD after ATP binding to TAP2 blocks conformational changes required for ATP binding to TAP1. To examine this assumption the rat TAP2 subunit was co-expressed with either human or rat TAP1 by rVV and binding of TAP to ATP-agarose was assessed in Ltk$^-$ versus Ltk$^-$-*US6* cells. As can be seen in Fig. 4.25 TAP complexes containing a human TAP1 subunit have a reduced capability of binding to ATP-agarose in the presence of gpUS6, whereas TAP complexes containing a rat TAP subunit have not. This finding indicates that binding of gpUS6 to TAP1 blocks conformational changes in *cis* essential for ATP binding to TAP1. Since rat TAP2 does not contain any binding sites for gpUS6, gpUS6 binding only to TAP1 is sufficient for the observed inhibition of ATP binding to TAP1.

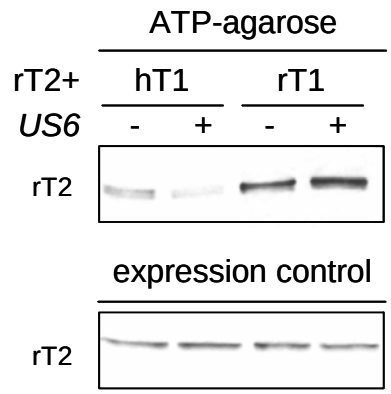

Fig. 4.25 gpUS6-mediated inhibition of ATP binding to TAP.

TAP subunits were expressed by rVV in Ltk$^-$ or Ltk$^-$-*US6* cells as indicated. At 6h p.i. cell lysates were prepared in ATP-binding buffer containing 1% digitonin. ATP-agarose was added and incubated for 30 min at 4° C. The agarose was washed and bound proteins were separated by 10% SDS-PAGE and transferred to a nitrocellulose membrane. Rat TAP2 was detected by D116 antiserum.

SUMMARY

- **ATP binding to TAP2 is absolutely required for gpUS6 recognition of TAP.**
- **gpUS6 recognition of TAP is independent of ATP binding to TAP1.**
- **gpUS6 senses conformational changes in the lumenal TMD induced by ATP binding to the TAP2 Walker A domain.**
- **gpUS6 binding to the TAP1 TMD blocks further TAP conformations required for ATP binding to the TAP1 NBD.**

4.7 Binding analysis of ICP47 to TAP

In contrast to gpUS6, the HSV encoded TAP inhibitor ICP47 is a small protein (8,5 kDa) that binds to TAP via the cytosolic face of the ER membrane. Since ICP47 prevents peptide binding to TAP, it was proposed that ICP47 associates with TAP at the peptide binding site, acting like as a high affinity competitor to peptide ligands (Ahn et al., 1996; Tomazin et al., 1996). As mentioned earlier, ICP47 has been shown to be species restricted (Jugovic et al., 1998). The determined affinity for human TAP is 50nM, whereas for mouse it is 100-fold lower (Ahn et al., 1996). Using the human and rat wt TAP subunits and intrachain chimeras it was aimed at defining TAP domains responsible for ICP47 interaction.

4.7.1 ICP47 binding to TAP is absolutely dependent on TAP2, but not sufficient for functional inhibition

First, human and rat wt subunits were expressed by rVV in TAP deficient CMT64.5 cells in addition to rVV co-expressing ICP47. ICP47 binding to TAP was demonstrated by co-IP of metabolically labeled TAP proteins by anti-ICP47 antibodies. In Fig. 4.26 clear precipitation of hTAP/hTAP2 can be observed. Co-expression of rat TAP subunits did not result in precipitation by ICP47. Combinations of human and rat subunits led to precipitation of TAP only in the presence of a human TAP2 subunit, i.e. human TAP1 combined with rat TAP2 is not recognized by ICP47. However, binding of ICP47 to rTAP1/hTAP2 was weaker than to hTAP1/hTAP2, suggesting that ICP47 binding to TAP is augmented by human TAP1.

For measuring of functional consequences of ICP47 interaction with TAP2, the human/rat TAP combinations described above were analyzed in peptide translocation assays. CMT64.5 cells were infected with TAP1 and TAP2 expressing rVV together with ICP47-rVV or a control virus. 75% of peptide translocation by hTAP1/hTAP2 was inhibited in the presence of ICP47 (Fig. 4.27). As expected, the rTAP1/rTAP2 and hTAP1/rTAP2 transporters were hardly affected by ICP47. Surprisingly, the ICP47 binding observed to rTAP1/hTAP2 did not lead to functional impairment of peptide translocation.

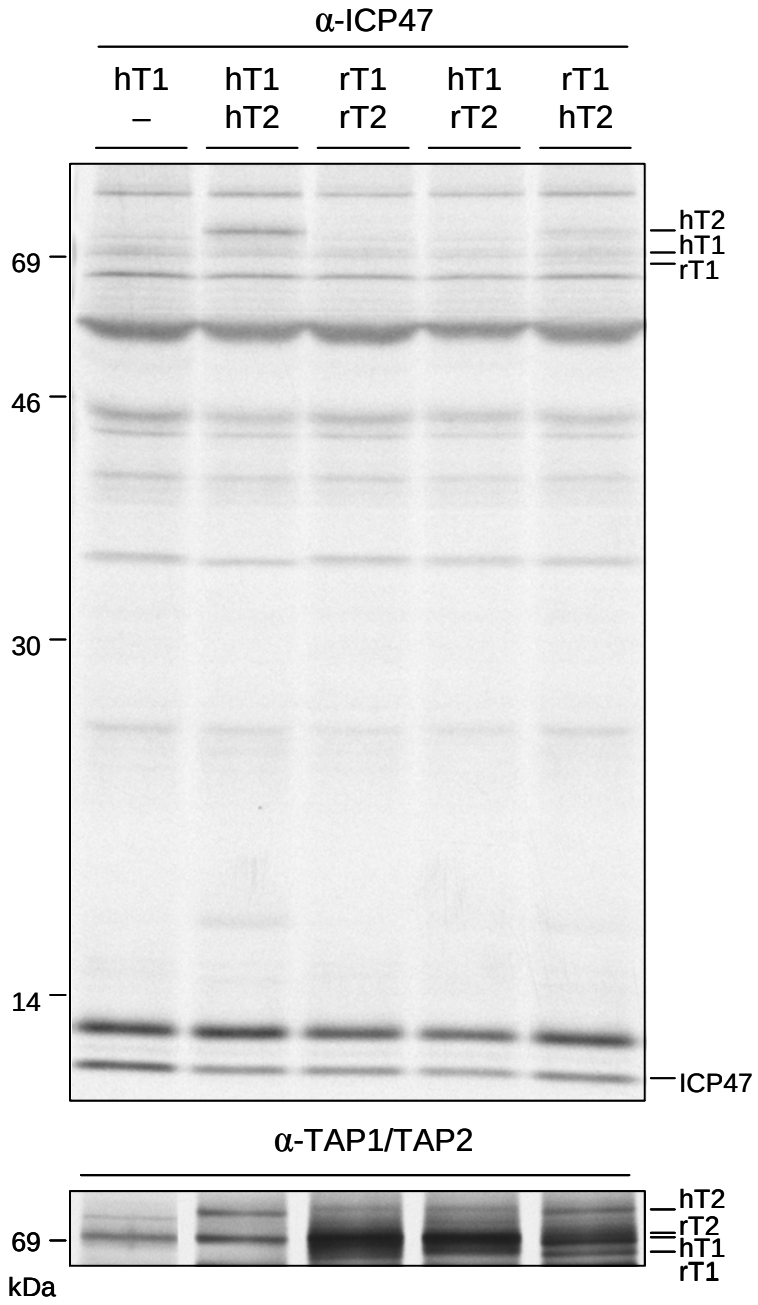

Fig. 4.26 Analysis of ICP47 binding to human TAP subunits.

Combinations of human and rat TAP subunits were co-expressed by rVV together with ICP47-rVV in CMT64.5 cells as indicated. At 15h p.i. binding of ICP47 to TAP was assessed by co-IP using anti-ICP47 antibodies (7µl 1361). Immunocomplexes were collected by PAS. Precipitated proteins were separated by a 10-13% gradient SDS-PAGE. The gel was dried and exposed to an autoradiography X-ray film for 24h. For expression control TAP subunits were precipitated as described in Fig. 4.20. The molecular weight marker is shown on the left side.

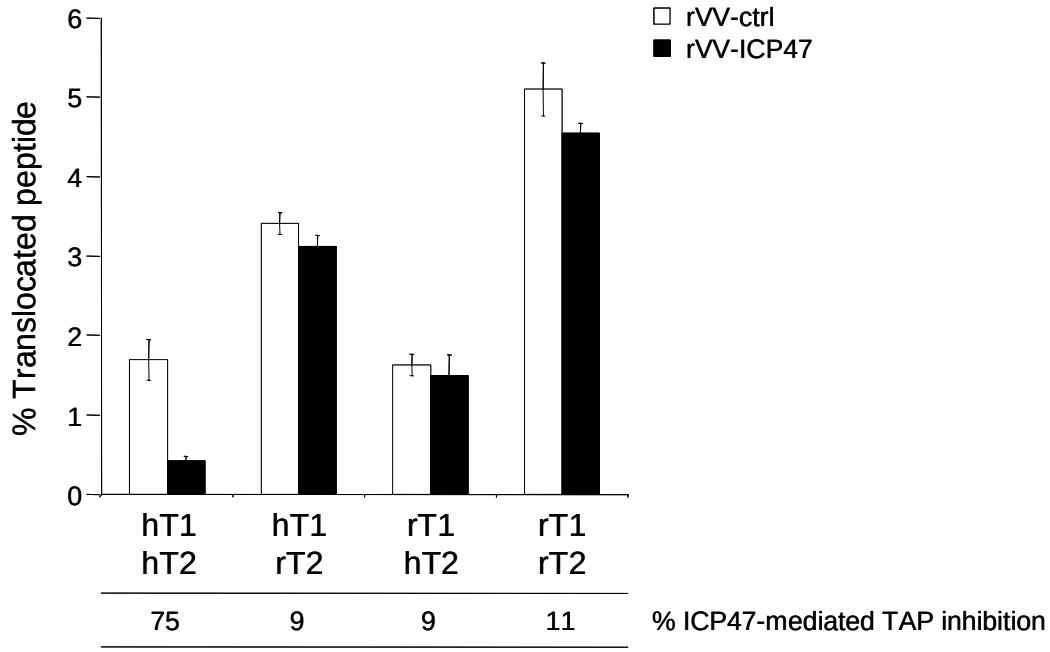

Fig. 4.27 ICP47-mediated inhibition of rVV-expressed TAP.

CMT64.5 cells were infected with rVV expressing TAP1 and TAP2 subunits together with ICP47-rVV (black bars) or a control virus (UL118-rVV) (open bars) as indicated with an MOI of 4. At 10h p.i. cells were permeabilized and peptide translocation was peformed as described in Experimental procedures. ICP47-mediated inhibition is expressed as the percentage of the difference of transport values in ICP47-rVV infected cells in comparison to ctrl-rVV infected cells.

4.7.2 ICP47 recognition of TAP2 is dependent on at least two independent domains

To define sequence requirements for ICP47 recognition of TAP2, the TAP2 human/rat chimeras (depicted in Fig. 4.17) were analyzed. The analysis was performed in CMT64.5 cells infected with TAP expressing rVV. The outcome of ICP47 binding to TAP2 chimeras combined with hTAP1 or rTAP1 is presented in Fig. 4.28. Surprisingly, ICP47 was found to bind to at least two independent sites on TAP2. The TAP2 mutants containing a human N-terminal TMD (h4rT2 and h7rT2) were both recognized by ICP47 in combination with a human TAP1 subunit (lanes 3 and 7). However, in combination with rat TAP1 the interaction with the N-terminal TMD was lost (lanes 4 and 8), although the expression control revealed high levels of TAP2 expression. Because rTAP1/hTAP2 complexes are recognized by ICP47, an additional interaction site to the one identified on h7rT2 must exist. This determinant is present on the chimera r4hT2, since this chimera was also precipitated by ICP47 in combination with rat TAP1 (lane 6). The chimera r7hT2 was not precipitated in combination with human TAP1 (the expression control shows that r7hT2 was expressed as strongly as

r4hT2), indicating that the additional ICP47 recognition site at the C-terminus of TAP2 is not formed when isolated from a human N-terminus. In conclusion, three domains on TAP2 were found to be important for effective binding of ICP47 to TAP: the N-terminal TMD (aa 1-177; defined by hT1/h4rT2), the central TMS (aa 178-363; defined by rT1/r4hT2) and the C-terminus of the TAP2 (C-terminal of aa 364; since rT1/r4hT2, but not rT1/h7rT2, is precipitated by ICP47). However, it is not possible to predict whether ICP47 interacts directly with the domains or if the domains are required for formation of the binding site. It would be very interesting to determine the contribution of these domains for the inhibition of peptide transport. This however, was not possible within the time constraints of the thesis.

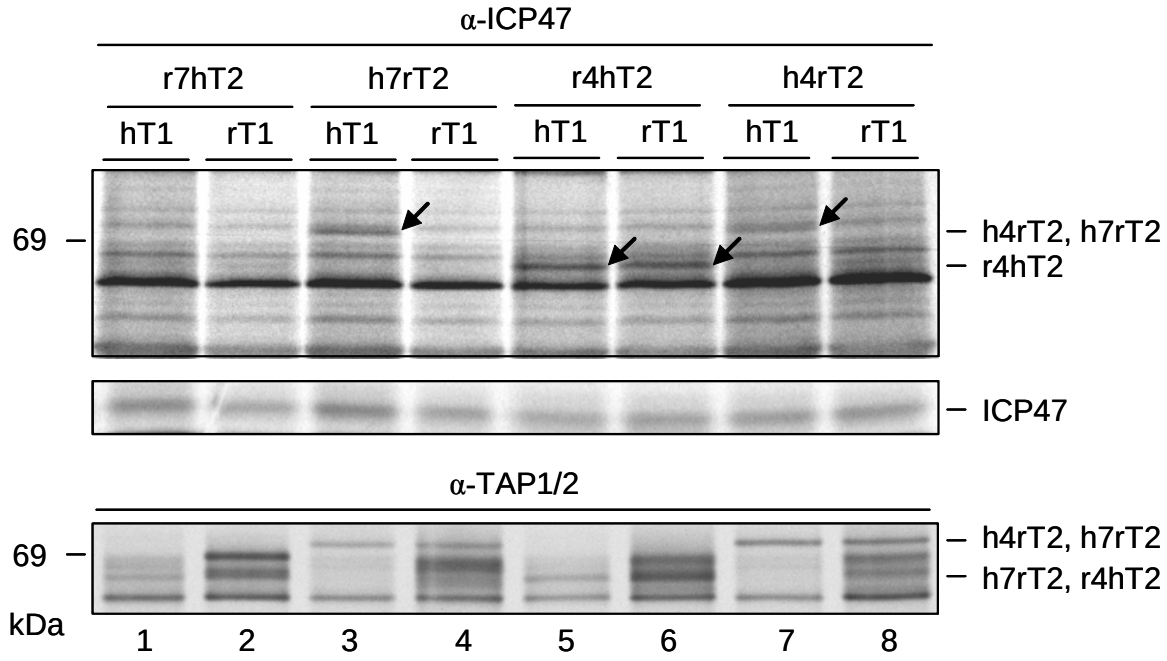

Fig. 4.28 Analysis of ICP47 binding to human/rat TAP2 chimeras.

Combinations of TAP subunits were co-expressed by rVV together with ICP47-rVV in CMT64.5 cells as indicated. Binding of ICP47 to TAP was assessed in metabolically labeled cells by co-IP using anti-ICP47 antibodies (7µl 1361). For expression control of TAP subunits hT1 was precipitated by 7505, rT1 by RatTAP1, h4rT2 and h7rT2 by RatTAP2 and r4hT2 and r7hT2 by TAP2.17. Immunocomplexes were collected by PAS (RatTAP1 and 2 antiserum by PGS). Precipitated proteins were separated by a 10-13% gradient SDS-PAGE. The gel was dried and exposed to an autoradiography X-ray film for 24h. The molecular weight marker is shown on the left side. The black arrows show specific precipitation of TAP subunits by ICP47.

SUMMARY

- **Both TAP1 and TAP2 contain sites important for ICP47 interaction, however, the initial ICP47 interaction with TAP is dependent on the TAP2 subunit.**
- **ICP47-mediated inhibition of peptide translocation requires interaction with both TAP subunits.**
- **Three distinct domains on TAP2 are involved in ICP47 interaction: the N-terminal TMD (depends on human TAP1), the central TMD (depends on human TAP1) and the C-terminus (independent of human TAP1 together with the central TMD)**

4.8 ICP47 recognizes an ATP-independent conformation of TAP

HSV1 encoded ICP47 does not prevent binding of ATP to TAP (Ahn et al., 1996; Tomazin et al., 1996). An interesting question was whether the Walker A TAP mutants influence ICP47 recognition of TAP. To investigate this the same setting as described for gpUS6 was used, co-expressing TAP Walker A mutants, wt subunits and ICP47 by rVV. Binding of ICP47 to TAP was analyzed by co-IP using anti-ICP47 antibodies. In contrast to gpUS6, ICP47 was able to precipitate all TAP1 and TAP2 Walker A mutants (Fig. 4.29). Only the weakly expressed T1Del was poorly precipitated in combination with TAP2. Therefore, ICP47 recognizes an ATP independent conformation of TAP.

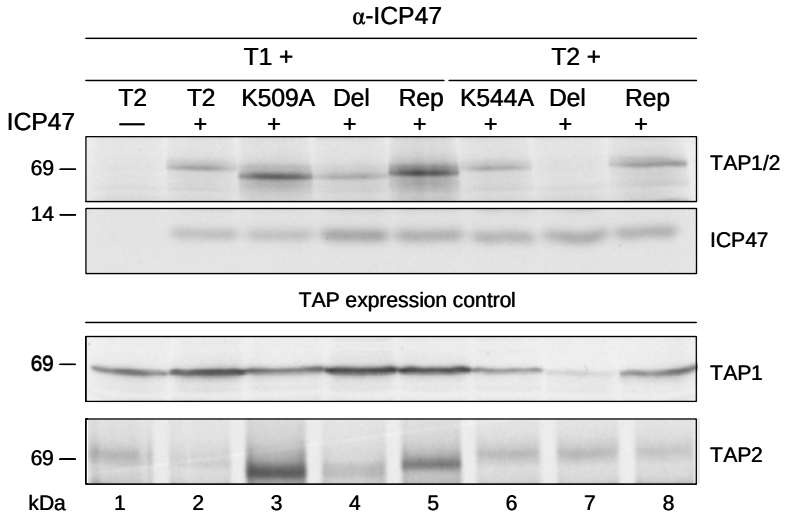

Fig. 4.29 Analysis of ICP47 binding to Walker A TAP mutants.

Human wt TAP1 was co-expressed with TAP2 Walker A mutants and the human wt TAP2 was co-expressed with TAP1 mutants in addition to ICP47 expression by rVV in CMT64.5 cells. Binding of ICP47 to TAP was assessed in metabolically labeled cells by co-IP using anti-ICP47 antibodies (7µl 1361). Immunocomplexes were collected by PAS. Precipitated proteins were separated by a 10-13% gradient SDS-PAGE. The gel was dried and exposed to an autoradiography X-ray film for 24h. The molecular weight marker is shown on the left side. For expression control TAP2 subunits were precipitated by TAP2.17 (2µl) and TAP1 was detected in Western blot by 148.3.

SUMMARY

- **ICP47 binding to TAP is independent of ATP induced TAP conformation.**

4.9 TAP binding by ICP47 and gpUS6 is mutually exclusive

The two viral TAP inhibitors gpUS6 and ICP47 share common features for TAP inhibition, i.e. interaction with both TAP subunits is a prerequisite for efficient inhibition of peptide translocation and they are species restricted. However, as demonstrated by the Walker A mutants, gpUS6 and ICP47 exert different requirements on TAP conformation. Whereas gpUS6 interaction with TAP is dependent on a functional TAP2 Walker A domain, ICP47 interacts with TAP independently of ATP. Accordingly, an interesting thought was to define if one of the inhibitors could adopt a dominant TAP conformation and prevent the other from recognizing its substrate. To approach the supposition HeLa cells tranfected with the genes for either *US6* or *ICP47* were used. Inhibitor expression and TAP inhibition by transfected genes were verified by extracellular staining of MHC class I molecules in FACS (Fig. 4.30). HeLa cells expressing gpUS6 or ICP47 showed a reduced level of MHC class I molecules on the cell surface, attributed to the inactivation of TAP dependent peptide translocation.

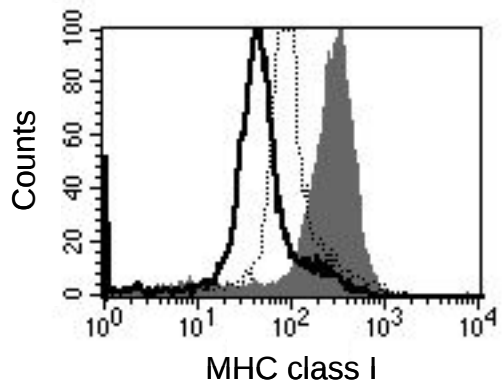

Fig. 4.30 MHC I cell surface expression of HeLa transfectants.

HeLa cells and stable HeLa transfectants expressing gpUS6 or ICP47 were stained for surface expression of MHC class I molecules by the antibody w6/32. FITC-labeled secondary antibody was used for visualization through FACS analysis. The grey surface corresponds to wt HeLa cells, the bold line to gpUS6 expressing cells and the dotted line to ICP47 expressing cells.

HeLa wild type cells and HeLa transfectants were infected with wt VV and rVV expressing gpUS6 or ICP47. TAP recognition by the inhibitors was assessed by co-IP of TAP by either anti-gpUS6 or anti-ICP47 antiserum. Co-IP and expression levels of TAP were detected by anti-TAP1 antibodies in Western blot. In *ICP47*-HeLa cells infected with gpUS6-rVV it was not possible to co-precipitate TAP by gpUS6 (Fig. 4.31, lane 5). This was surprising since in *US6*-HeLa cells infected with ICP47-rVV TAP was clearly co-precipitated by anti-gpUS6

antibodies (lane 4), although gpUS6 levels were much lower. Conversely, when co-precipitating TAP by anti-ICP47 antibodies, the occurring pattern was reverse: in cells transfected with *ICP47* TAP was clearly recognized by ICP47 (lane 7-9), but if ICP47 was expressed later than gpUS6, ICP47 was not able to associate with TAP (lane 10). Interestingly, both viral inhibitors prevent binding of the other inhibitor to TAP, i.e. gpUS6 and ICP47 are mutually exclusive. gpUS6 and ICP47 freeze the TAP complex in an unfavorable conformation for the other inhibitor, which reveals an intramolecular crosstalk of TAP TMDs and NBDs that determines TAP conformations.

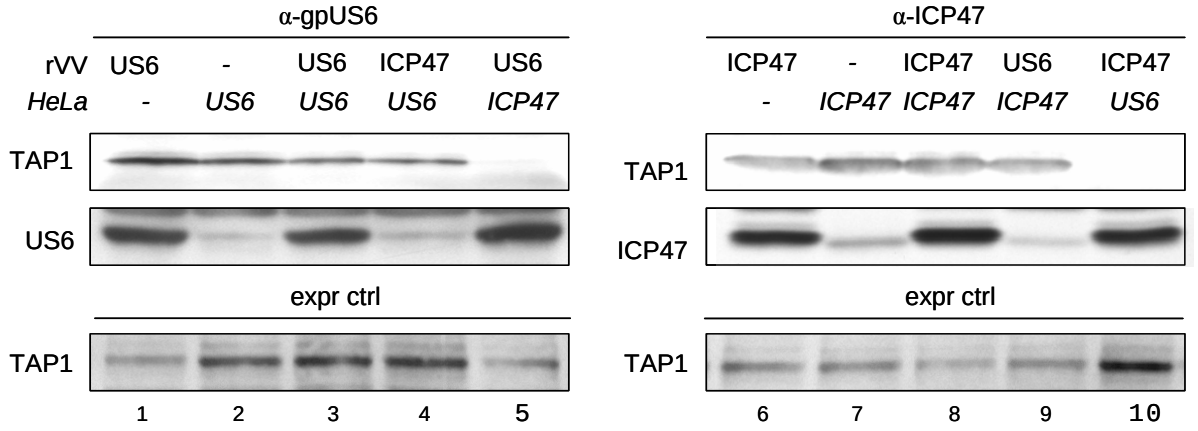

Fig. 4.31 TAP precipitation from HeLa cells expressing gpUS6 and ICP47.

HeLa cells transfected with the genes for ICP47 or gpUS6 were infected with rVV expressing ICP47 or gpUS6. Cell lysates were prepared with IP lysis buffer containing 1% digitonin and TAP complexes were precipitated by anti-gpUS6 or -ICP47 antibodies (7510 or 1361, respectively). After collection of immunocomplexes by PAS, proteins were separated by 10% SDS-PAGE and transferred to a nitrocellulose membrane for detection by Western blot. The membrane was cut in two parts, one above the 50 kDa marker band for detection of hT1 by 148.3 and one below for detection of gpUS6 by 7510 antiserum. For ICP47 detection, cells were metabolically labeled and ICP47 was precipitated from cell lysates by 1361 and detected after SDS-PAGE as described in Fig. 4.29. For control of hT1 expression, an aliquot of each lysate was analyzed by Western blot.

SUMMARY

- **Binding of ICP47 and gpUS6 to TAP is mutually exclusive.**
- **ICP47 binding to TAP is not independent of TAP conformation.**
- **TAP inhibitors prove intramoleular crosstalk between lumenal TMDs and cytosolic NBDs of TAP.**